

DEPOLARISATION CHARACTERISTICS IN SOL-GEL DERIVED LEAD ZIRCONATE TITANATE THIN FILMS

*A Thesis Submitted in Partial Fulfilment of
the Requirements for the Degree of*
MASTER OF TECHNOLOGY

By
V. Ramesh

Material Science Programme
Indian Institute of Technology, Kanpur
June 1996

2 1996 / M.S.P

CENTR

RY

Acc. No

122557



A122557

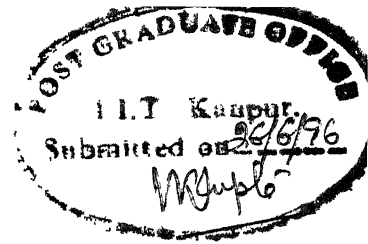
4897

MSP-1996-M-RAM-DEP

To


My

Parents




CERTIFICATE

This is to certify that the work presented in this thesis entitled, "DEPOLARIZATION CHARACTERISTICS IN SOL-GEL DERIVED LEAD ZIRCONATE TITANATE THIN FILMS" by *V. Ramesh* is a record of work carried out under our supervision and it has not been submitted elsewhere for a degree.


(D.C. Agrawal)

Materials Science Programme,
I.I.T., Kanpur.


(Y.N. Mohapatra)

Materials Science Programme
I.I.T., Kanpur.

June, 1996.

ERRATA

1. Page (ii), paragraph-1: *changed applying* to be read as *changed by applying*
- 2 Page (iv): $Pb(Zr_{0.53}Ti_{0.47})O_3$ to be read as $Pb(Zr_{0.53}Ti_{0.47})O_3$
3. Page 5, paragraph-1: *m1attempt* to be read as *major attempt*
4. Page 9, paragraph-2: *extensive of* to be read as *extensive study of*
- 5 Page 16: $Pb(Zr_{0.53}Ti_{0.47})O_3$ to be read as $Pb(Zr_{0.53}Ti_{0.47})O_3$
6. Page 17: Al_2O_3 to be read as Al_2O_3
7. Page 29, paragrph-1: (*cf. §2 5*) to be read as (*cf. §2.3 2*)

ABSTRACT

Thin films of lead zirconate titanate (PZT) have emerged as an important material for applications based on their ferroelectric, pyroelectric and piezoelectric properties. One of the recent applications, which has attracted lot of attention and effort, is in non-volatile computer memories based on the reversibility of polarisation state. However, there are several material related problems which have to be solved before widespread technological adoption is possible. As far as memory applications are concerned, there are two such important degradation related problems known as fatigue and depolarisation. Fatigue, the degradation of switchable polarisation with number of switching cycles, has been studied in detail by many workers. On the other hand depolarisation, defined as short time retention of polarisation, is not well studied. In the present work, we study the depolarisation behaviour in sol-gel derived PZT thin films.

Thin films of composition $Pb_{1.05}(Zr_{0.53}Ti_{0.47})O_3$ in the thickness range $0.8 - 1.25\mu m$ have been prepared using sol-gel technique on Pt substrates. Two different heat treatments were employed in preparing the samples. Films which are fired at $400^\circ C$ and annealed at $700^\circ C$ are termed as slow fired samples and those fired at $600^\circ C$ and annealed at $700^\circ C$ are termed as fast fired samples. Routine characterisation of the samples have been carried out using XRD, C-V and P-E measurements.

The depolarisation behaviour of PZT thin films have been studied using a new measurement sequence which consists of following steps: (i) Polarising the sample to the desired polarisation state utilising P-E measurements, (ii) Switching or reinforcing the polarisation state by applying a square voltage pulse (iii) Monitoring the polarisation as a function of time thereafter. Hysteresis loops have been recorded at various steps to observe any possible changes in the loops parameters. The depolarisation characteristics have been measured with respect to pulse height (15–20V),

pulse width (3–30s) and temperature.

The hysteresis loops obtained from PZT capacitors exhibited asymmetry along the field axis indicating the presence of internal bias E_i which favours a definite polarisation state in the sample. We show that internal bias can be changed applying an external voltage pulse. We further show that there exists a definite relationship between achieved polarisation state and the final orientation of internal bias E_i . In our measurements, we not only observed loss of polarisation but also backswitching of polarisation state.

We have used an isothermal technique called time analysed transient spectroscopy (TATS) to analyse the polarisation decay curves. It is found that decay of polarisation is exponential and the time constant are calculated from TATS. There is a sample to sample variation of observed time constants and this is attributed to inhomogeneous distribution of species producing the depolarising field. From the exponential nature of decay of polarisation, it has been concluded that the value of opposing depolarising field remains constant in the absence of external voltage.

Our measurements with respect to pulse height, pulse width and temperature indicated that depolarisation behaviour is independent of these parameters. It is found that the values of internal bias E_i obtained from low frequency measurements (0–4Hz) are influenced by measurement sequence itself but the orientation of E_i is not affected.

We have considered three existing models in the literature and found that they are unable to explain some of our crucial observations such as exponential nature of polarisation decay and backswitching of polarisation states. We propose a new model based on the depolarising field arising from the asymmetry of charge distribution in the interfacial space charge regions, due to trapping(detrapping) of charge carriers while applying an external voltage pulse.

Acknowledgements

I pay my respects to my thesis supervisors Prof. D.C. Agrawal and Dr. Y.N. Mohapatra for introducing me to the field of electronic ceramics and for their constant encouragement throughout the course of this work. I specially thank Dr Mohapatra for long hours of enchanting discussions which I had with him.

I wish to thank my labmate Subhashish for his valuable suggestions in all my experiments and for discussions which I had with him. I wish to thank him for his encouraging words and brotherly advice which is always motivating. I wish to thank my labmates Atanu, Ajay Garg, Shantanu for their kind advice and love towards me. I also wish to thank Subhash for the care which he has taken towards me. I wish to thank my other labmates Sangita, Archanaji, Giriji, Puthal and Gurvinder for their ever smiling faces.

I am grateful to Joginder for his help in preparing this thesis in many ways. I specially thank him for introducing me to Vedanta. The long hours of discussions which I had with him in this regard are sweet memories of our days spent together.

I wish to thank my other batchmates Roy, Madhukar and Rajput for nice time I had with them. I also wish to thank my Tamil friends for their love towards me and for nice lawn chats.

I have best regards for my hostel friends Venkat, Kamal(Rambabu), Sushil, Govind, Chaveli, Tiwari, Sundar, Sudipto and Anand. I owe many lively moments to them.

I also pay my respects to Dr. T.V. Prabhakar and Mataji (Mrs. Prabhakar) for their love towards me.

Finally, I wish to thank all my family members especially my brothers for their constant source of encouragement throughout this work.

Contents

| | | |
|----------|---|-----------|
| 1 | Introduction | 1 |
| 1.1 | Ferroelectric Ceramics | 2 |
| 1.2 | Lead Zirconate Titanate (PZT) | 2 |
| 1.3 | Ferroelectric Thin Films | 3 |
| 1.4 | Preparation Techniques of Ferroelectric Thin Films | 4 |
| 1.5 | Motivation of this Work | 5 |
| 1.6 | Depolarisation Studies: A Brief Review | 6 |
| 1.7 | Definition of the Problem | 13 |
| 2 | Experimental Details | 14 |
| 2.1 | Introduction | 14 |
| 2.2 | Sol-Gel Method | 15 |
| 2.3 | Preparation of $Pb(Zr_{0.53}Ti_{0.47})O_3$ Thin Films | 16 |
| 2.3.1 | Spin Coating | 18 |
| 2.3.2 | Firing and Annealing | 20 |
| 2.4 | Experimental Details | 23 |
| 2.4.1 | Experimental Set-Up For Hysteresis Measurements | 23 |
| 2.4.2 | Description of Set-up For Depolarization Measurements | 24 |
| 2.4.3 | Description Of The Sample Holder | 25 |

| | | |
|----------|---|-----------|
| 3 | Measurements and Results | 28 |
| 3.1 | Sample Details and Standard Characterization | 28 |
| 3.2 | Polarisation - Electric Field Measurement | 29 |
| 3.3 | Capacitance – Voltage Measurements | 33 |
| 3.4 | Depolarisation measurements | 34 |
| 3.4.1 | Description of the Measurement Sequence | 34 |
| 3.4.2 | Description of the General Behaviour of the Depolarisation Characteristics | 37 |
| 3.5 | Depolarisation Measurements on the Fast Fired Sample | 41 |
| 3.5.1 | Dependence of the Depolarisation Characteristics on the Mag- nitude of the Applied Voltage Pulse | 41 |
| 3.5.2 | Dependence of Depolarisation on the Width of the Applied Voltage Pulse | 44 |
| 3.5.3 | Back Switching and Decay Time Constant | 45 |
| 3.5.4 | Repeatability of Depolarisation Behaviour | 49 |
| 3.5.5 | Temperature Dependence of Depolarisation | 52 |
| 3.6 | Depolarisation Measurements on the Slow Fired Sample | 55 |
| 3.7 | Temperature and Electric field Dependence of Internal Bias E_i | 58 |
| 3.8 | Influence of P–E Measurements on Internal Bias | 59 |
| 4 | Discussion | 63 |
| 4.1 | Critical Comparison of existing Models | 67 |
| 4.1.1 | Capacitor Models | 67 |
| 4.1.2 | Defect Dipole Model | 69 |
| 4.1.3 | Proposed Model For Depolarisation | 70 |
| 5 | Summary and Conclusions | 76 |

5 1 Scope For Future Work 79

List of Figures

- 1.1 Schematic of pulse sequence adopted by Benedetto et al.
- 1.2 Schematic of pulse sequence adopted by Mihara et al.
- 1.3 Schematic of normal and modified hysteresis loops.
- 1.4 Schematic of model proposed by Mihara et al.
- 2.1 Flow Diagram of substrate cleaning procedure.
- 2.2 Schematic of heat treatment for slow fired sample.
- 2.3 Schematic of heat treatment for fast fired sample.
- 2.4 Flow diagram for preparation of PZT films.
- 2.5 Schematic of Sawyer-Tower circuit.
- 2.6 Schematic of implementation of Sawyer-Tower circuit.
- 2.7 Schematic of sample holder used for P-E measurements.
- 2.8 Schematic of sample holder used for electron-emission experiments.
- 3.1 Hysteresis loop of slow fired sample.
- 3.2 Hysteresis loop of fast fired sample.
- 3.3 Hysteresis loop showing relationship between E_s and sign of saturation of polarisation.
- 3.4 Hysteresis loop showing relationship between E_s and sign of saturation of polarisation.
- 3.5 C-V characteristics of Fast fired sample.
- 3.6 Schematic of four different regions of depolarisation characteristics.
- 3.7 Schematic of TATS signal.
- 3.8 Depolarisation behaviour of -Pr:S.C in fast fired Capacitor 1.
- 3.9 Depolarisation behaviour of -PR:N.S.C in fast fired Capacitor 1.
- 3.10 Depolarisation behaviour of +Pr:S.C in fast fired Capacitor 1.

- 3 11 Depolarisation behaviour of +Pr:N.S.C in fast fired Capacitor 1.
- 3 12 Depolarisation behaviour of -Pr:S.C in fast fired Capacitor 2.
- 3.13 Depolarisation behaviour of +Pr:N.S.C in fast fired Capacitor 3.
- 3.14 Depolarisation behaviour of +Pr:S.C in fast fired Capacitor 3.
- 3.15 Depolarisation behaviour of -Pr S.C in fast fired Capacitor 3.
- 3.16 TATS signal for +Pr:N S.C in fast fired Capacitor 3.
- 3.17 TATS signal for +Pr:S.C in fast fired Capacitor 3
- 3.18 TATS signal for -Pr:S.C in fast fired Capacitor 3.
- 3.19 Depolarisation behaviour of -Pr:S.C of fast fired Capacitor 4.
- 3.20 Depolarisation behaviour of -Pr:N.S.C of fast fired Capacitor 4.
- 3.21 Depolarisation behaviour of +Pr:S.C of fast fired Capacitor 4.
- 3.22 Depolarisation behaviour of +Pr:N.S.C of fast fired Capacitor 4.
- 3.23 Depolarisation behaviour of -Pr:S.C of fast fired Capacitor 4 with varying temperature.
- 3.24 Depolarisation behaviour of -Pr:S.C of fast fired Capacitor 4 at 115 C.
- 3 25 Depolarisation behaviour of +Pr:N.S.C in slow fired sample.
- 3 26 Depolarisation behaviour of +Pr:S.C in slow fired sample.
- 3.27 Depolarisation behaviour of -Pr:N.S.C in slow fired sample.
- 3 28 Schematic of influence of measurement sequence on E_i .
- 4 1 Schematic illustrating orientation of E_i and Pr inside the sample.
- 4.2 Schematic illustrating different magnitudes of E_i .
- 4.3 Schematic illustrating origin of E_i .
- 4.4 Schematic of Auger data obtained on PZT films by Scott et al.

List of Tables

- 2 1 List of chemicals used to prepared the sol.
- 3.1 Four cases of switching and non-switching of sample polarisation.
- 3.2 Results of depolarisation measurements with pulse height = 15V.
- 3.3 Results of depolarisation measurements with pulse height = 20V.
- 3.4 Results of depolarisation measurements with various pulse widths.
- 3.5 Results of depolarisation measurements–Backswitching nature.
- 3 6 Results of depolarisation measurements–Repeatability.
- 3 7 Results of depolarisation measurements–Repeatability.
- 3.8 Results of depolarisation measurements–Temperature dependence.
- 3.9 Results of depolarisation measurements on slow fired sample.
- 3 10 Results indicating independence of internal bias on applied field.
- 3 11 Results indicating dependence of internal bias on temperature.

Chapter 1

Introduction

Ferroelectricity, the reversal of spontaneous polarisation by the applied electric field, was discovered by Valasek in Rochelle salt (Sodium potassium tartrate) in 1923. After this discovery, ferroelectricity was reported in many more crystals like KDP (Potassium dihydrogen phosphate), ADP (Ammonium dihydrogen phosphate) etc. But, significant breakthrough in understanding the structural origin of ferroelectricity came through the discovery of the same in $BaTiO_3$ in 1945. The large dielectric and piezoelectric constant of ferroelectrics immediately made these materials attractive candidates for a variety of applications. For many years, ferroelectrics dominated the field of sonar detectors, phonograph pickups and so on. Pyroelectric properties of these materials are utilised in fabrication of devices such as IR detectors etc., However none of these devices directly utilised the ferroelectric nature of the material, namely large reversible spontaneous polarisation. In the recent years this switchability of the polarisation has been demonstrated to have applications in non-volatile memories for computer systems. Since then many laboratories all over the world are engaged in solving problems related to applications involving polarisation reversal. In this thesis we investigate one aspect of ferroelectric capacitors

directly relevant to such applications. Before stating our problem, we introduce the necessary concepts briefly in the following sections.

1.1 Ferroelectric Ceramics

For the study of the fundamental properties of the ferroelectric materials initially single crystal samples were used because they provide the advantage of having less imperfections and surface effects. Ferroelectric ceramics, on the other hand have the advantage of being a great deal easier to prepare than their single crystal counterparts. In many cases, they show ferroelectric properties approaching quite closely to those of the single crystals. In addition, it is possible to prepare wide range of ceramic compositions and to tailor the characteristics of the material properties for different applications.

1.2 Lead Zirconate Titanate (PZT)

Of many known ferroelectric ceramics lead zirconate titanate (PZT), a solid solution obtained from lead zirconate and lead titanate, has attracted the attention of the researchers because of its potential applications as pyroelectric detectors, piezoelectric transducers and in opto-electronic devices. The PZT ceramics are chemically represented by $Pb(Zr_xTi_{1-x})O_3$. They are perovskite solid solutions of antiferroelectric $PbZrO_3$ and ferroelectric $PbTiO_3$ and can exist in any of three crystal structures: tetragonal, rhombohedral and orthorhombic. Above a certain temperature called Curie temperature, the ceramic has a cubic structure and is paraelectric. On cooling below the Curie temperature, the phase transformation to tetragonal or rhombohedral structure depending upon the composition occurs. To minimise the accompanying stresses, each grain of the ceramic breaks into domains. In a do-

main the polarisation is directed along the crystallographically allowed directions. The net polarisation in the ceramic due to random orientation of domains is zero. When a sufficiently high electric field is applied, the domain tends to align along the field direction and the ceramic attains a net polarisation. This process is called poling. In PZT ceramics, a sharp phase boundary between the rhombohedral and the tetragonal phase called the morphotropic phase boundary (MPB). exists at the composition $Pb(Zr_{0.53}Ti_{0.47})O_3$. The composition in the MPB region are of immense of technological importance because of high values piezoelectric coefficients, large remanent polarisation and reasonable coercive field etc. The sample used in this work are prepared with their composition near MPB.

1.3 Ferroelectric Thin Films

The first report of ferroelectric thin film growth involved the materials of perovskite structure. In 1955 Feldman [1] reported the synthesis of micrometer thick $BaTiO_3$ on Pt by flash evaporation. These films were amorphous as-deposited and had to be heated to above 1100° C to obtain polycrystalline films with a low dielectric constant. Later Moll [2] and Muller et al from Philco Scientific Labs., used a grain by grain evaporation technique to attempt a epitaxial growth. Muller et al[3] reported the first successful vapour growth of epitaxial films of a wide variety of simple perovskites on LiF heated to about 600°C. In beginning of 1970 synthesis was dominated by the newly developed rf sputtering technique. The capabilities of obtaining desired properties in thin film significantly widens the scope of applications. Rapid progress has been made in thin film devices in the last decade.

1.4 Preparation Techniques of Ferroelectric Thin Films

In general, film deposition techniques can be divided into dry and wet processes. The dry process includes sputtering, evaporation, whereas the common wet processes are Metallo-Organic Deposition (MOD) and sol-gel. The wet processes usually use unheated substrates or low temperature deposition, whereas dry processes use a range of temperatures, typically unheated substrates to 700°C. As an example, MOCVD is done at elevated temperature due to the necessity of hot substrate surface for condensing films. On the other hand, sol-gel film deposition is usually done on unheated substrates. With exception of MOCVD, all other dry processes involve physical vapour deposition (PVD). The major PVD techniques differ among themselves in several ways, particularly in the energetics of the flux incident on the substrate during film growth. Techniques such as, rf-sputtering and ion beam sputtering tend to have large amounts of energetic species incident on the growing film due to large target voltages, whereas evaporation usually involves very small energy flux at the substrate. Laser deposition and magnetron sputtering involve intermediate level of energetic bombardment of the substrate. All these techniques have been successfully used to prepare PZT thin films. However, among these techniques sol-gel route is probably the best as regards to formation of perovskite phase, homogeneity of composition and control over thickness. In this work we use exclusively sol-gel route to prepare the films. Sample preparation details are given in Chapter 2.

1.5 Motivation of this Work

In this section we provide only a broad motivation behind this work, leaving the precise definition of the problem to a later section. One recent application of PZT thin films is their usage in non-volatile computer memories based on their bistable polarisation state which can be switched from one state to another by applying an external voltage. An attempt was made in the 1950's and 60's by several researchers in this direction. But at that time one of the major obstacle was the lack of proper deposition technique that could achieve high quality sub-micron ferroelectric thin films. Earlier ferroelectric memories[4] employed bulk material that resulted in switching threshold of the order of tens or hundreds of volts. and the switching speeds in the range of microseconds to milliseconds, rendering the technology incompatible with the silicon IC technology.

However, with the advent of modern thin film deposition techniques to produce sub-micron ferroelectric thin films, the above mentioned problems have been solved. David Bondwani[5] fabricated a FERAM (Ferroelectric Random Access Memory) with 64k memory. FERAM's with higher memory capacities were also reported in the literature[6]. But, the commercial viability of these memories is dictated not only by the cost but also by their longterm time performance. There are several phenomena which degrade the properties of a ferroelectric capacitor used as a memory cell. Among them fatigue is the degradation of the sample polarisation by repeated switching and it has been studied by many authors in some detail[7]. The phenomenon of depolarisation is defined as short time retention property in the literature[8]. There is a related phenomenon, referred to as imprint by some authors[9], in which the sample capacitor develops a tendency to favour a preferred polarisation state. Though imprint itself is defined as a separate phenomenon, the exact demarcation line between these two properties, viz., depolarisation and im-

print, is not quite clear. In this work, we have confined to study the phenomenon of depolarisation in great detail to bring the possible mechanisms responsible for it.

1.6 Depolarisation Studies: A Brief Review

To the best of our knowledge, there are only two reports exclusively devoted to depolarisation phenomenon in PZT thin films by Benedetto et al[10] and Mihara et al [8]. Benedetto et al studied the effects of operating conditons on the fast decay component of the retained polarisation in PZT thin films. They simulated the write (read) conditions that would be experienced by the ferroelectric film in a non-volatile memory circuit. In a memory element a data bit ('1' or '0') will be stored and available for query at some later time. During a read the memory element must be able to respond with the proper state in a time scan from few hundred nanoseconds upto full year or more after the write pulse.

The measurement sequence used in their work consists of short square voltage pulses for both storing data bits (write pulse) and for querying the stored values (read pulse). Write pulses are positive to store a '1' and negative to store a '0' and read pulses are always positive (arbitrary convention) . The schematic of the pulse sequence used by Benedetto et al is shown in Fig. 1.1. The signals generated during the read voltages to indicate the memory state are voltages appearing across the sense capacitor of the Sawyer-Tower circuit. For a stored '1' a relatively small voltage appears across the sense capacitor and for stored '0' a relatively high voltage appears. The difference in the voltage in these two cases is the "Memory window", that enables the memory circuit to distinguish between '0' and '1'. The difference between these two cases is termed as the retained polarisaion i.e., the retained polarisation = memory window. The decrease of memory window is monitored as a

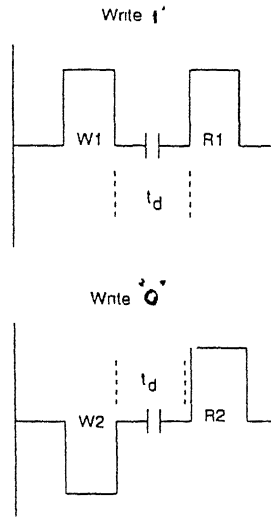


Fig 1.1 Pulse Sequence adopted By
Benedetto et al For Depolarisation Study

function of time delay t_d between the write and read pulses

Using this basic approach for measuring the retained polarisation, they varied several parameters to investigate the mechanisms involved in the fast decay of remanent polarisation. The parameters varied are write (read) pulse amplitude, write (read) temperature and the number of fatigue cycles experienced by the sample. The samples used for their work were 200nm thick Sol-Gel derived PZT (40/60) capacitors with Pt top electrodes and non-patterned bottom electrode.

The polarisation decay was measured at three different write (read) voltage levels (3.5V, 5.0V and 7.7V). From the results of the measurements it has been concluded that neither the relative fraction of loss of initial polarisation nor the time scale for the decay are significantly dependent on the magnitude of the pulses used to write and read. i.e., the magnitude of the time dependent retained polarisation simply scales along with the initial polarisation.

The polarisation decay was measured at two levels of fatigue ($< 10^4$ switching

cycles and 2×10^8 switching cycles). A bipolar square wave of $\pm 5\text{V}$ at a rate of 333kHz was used to apply the switching cycles. In the fatigued samples the percentage of loss of polarisation has changed, but the exact nature of the change has not been reported. Benedetto et al emphasize the requirement of more data in this regard before making any definite correlation.

The nature of the polarisation decay was studied at room temperature and at 125°C . The measurements at 125°C indicated higher initial rate of decay than it was in the room temperature measurement. But, Benedetto et al emphasize the requirement of more data for making any definite correlation.

Based on their experiments, Benedetto et al propose a model to explain the fast decay component of polarisation. In this model the results of the fatigue and temperature measurements were not taken into account. According to their model time dependent depolarisation fields cause the partial reversal of polarisation. Benedetto et al explain their model as follows: To some extent depolarisation fields always exist in thin insulating ferroelectric thin films due to extent of finite separation between the polarisation charge and the compensating free charges in the electrode²¹[?]. If the polarisation is essentially constant upto the immediate vicinity of the electrodes then depolarisation fields are generally small. However, if a gradient in the polarisation exists over some appreciable distance near the electrode interfaces or if the compensating charges in the electrodes is distributed over a finite screening distance or especially if there are non-switching layers in the ferroelectric film near the interfaces then the depolarisation fields may be significant. Indeed since the depolarisation fields are in a direction opposite to that of the bulk polarisation, partial reversal of polarisation may occur if the magnitude of depolarisation field exceeds the coercive field. In turn, the depolarising fields relax as the reverse switching occurs with the process ceasing when depolarising field drops approximately to the

value of coercive field

Benedetto et al obtained only the quantitative loss of polarisation with different time delays between the read and write pulses, but the exact nature of decay of polarisation in this time interval was not studied.

Mihara et al [8] carried out an extensive of depolarisation behaviour in sol-gel derived PZT by utilising four consecutive positive pulses instead of conventional positive and negative double pulses. The schematic of pulse sequence adopted by Mihara et al is shown in Fig. 1 2. The normal hysteresis loop and modified hysteresis loop to explain the proposed depolarisation are given in Fig. 1 3, where P_r and P_s represent remanent and saturation polarisation respectively and subscripts + and - represent the polarity. In Fig. 1 2 notations A to D show the path of the hysteresis loop corresponding to the pulse train being evaluated. The trace passes from A to C, when the polarisation is switched. After the polarisation switching and pulse has fallen to zero, the state C is assumed, to transit to the relaxation point D. For a non-switched pulse, the trace passes from D to C through B. Consequently P_{r+}^{\wedge} is observed as the difference between the C and D, which is assumed to transit after the pulse falls to zero. The parameter P_{r+}^{\wedge} is defined as the depolarisation parameter by Mihara et al. Extended evaluations were carried out for pulse height, pulse width, temperature dependence and space charge effect.

The depolarisation parameters are measured by changing the width and height of the pulses. The pulse height was changed from 3V to 8V and they found that depolarisation parameter P_{r+}^{\wedge} is independent of pulse height. The width of the pulses are changed from 1–100 μ s. In this case the depolarisation parameter is found to be independent of pulse width. From these measurement they concluded that depolarisation is not governed by an unsaturated polarisation at first read pulse.

A possible depolarisation mechanism is trapping (detrapping) of carriers to

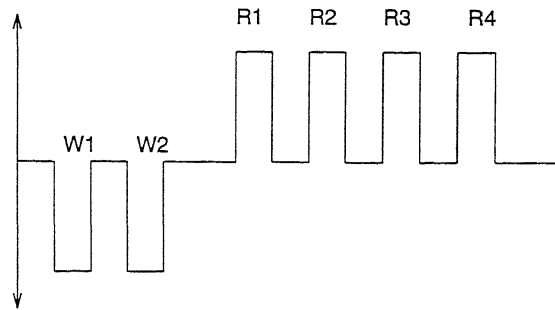


Fig. 1.2 Pulse Sequence adopted By Mihara et al For Depolarisation Study

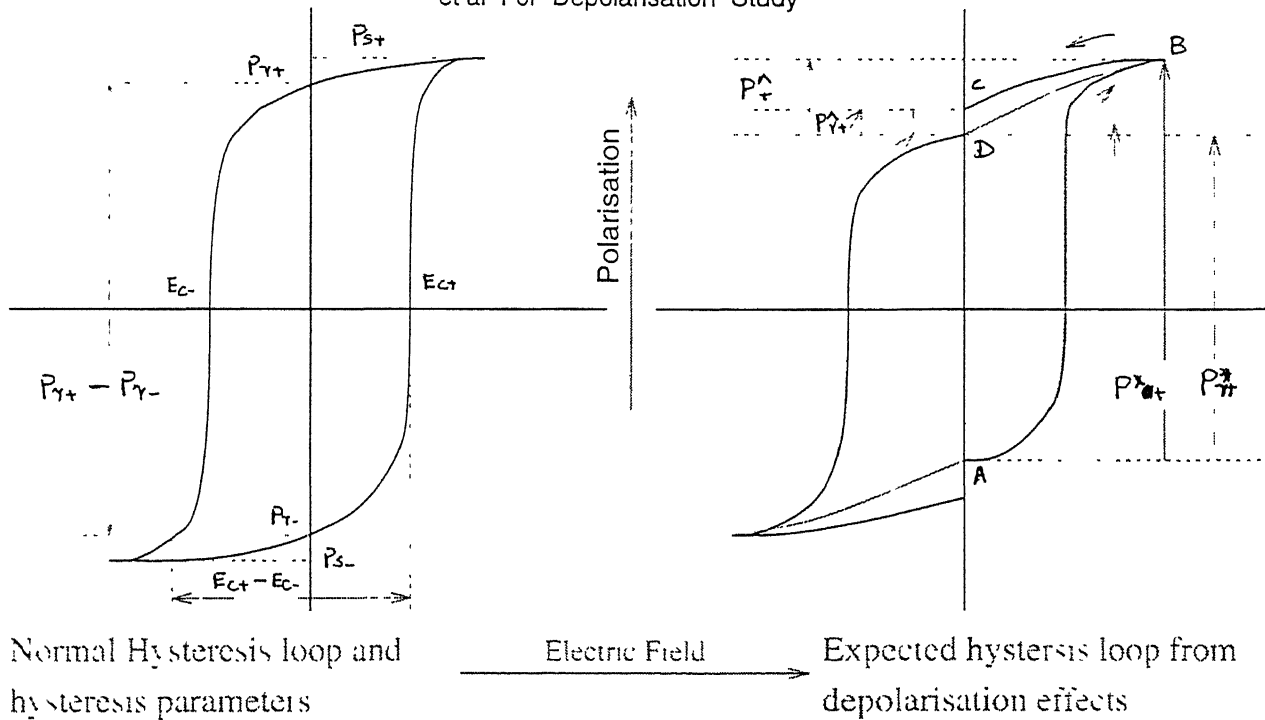


Fig. 1.3 Schematic Showing Normal Hysteresis Loop And Expected Hysteresis Loop From Depolarisation Effects
(Ref. Mihara et al)

(from) space charges in ferroelectrics. To clarify this effect, the depolarisation parameter is studied as a function of temperature. The depolarisation parameter P_{r+} did not change in the temperature range from 20 – 160°C. The depolarisation parameters are also studied as a function of excess lead in the stock solution which is used to prepare PZT thin films. The depolarisation parameter did not change significantly with excess lead %. Hence, they concluded that space charge effects have no influence on the depolarisation mechanism. However, we feel that rejection of space charge model is not fully warranted.

Based on their measurements, Mihara et al propose a model for depolarisation by attributing the origin of depolarisation field to the standard capacitor connected to the sample in depolarisation measurements. This field is called external depolarisation field $E_d(ext)$. When the input voltage V_{in} goes to zero, the top plate of the standard capacitor is still at higher potential and hence produces an depolarisation field. But, the depolarisation phenomenon has been reported in resistor loaded circuits also. In this case Mihara et al explain the depolarisation on the basis of an interfacial capacitor in the sample and this interfacial capacitor is similar to that of model proposed by Benedetto et al. The schematic of the model is as shown in Fig. 1.4.

The measuring circuit which is used by Mihara et al is conventional Sawyer-Tower circuit[11]. One essential requirement of this circuit is that the value of the standard capacitor used in this circuit should be very large compared to the sample capacitance. But, the standard capacitor used by Mihara et al has a ratio of only 20 with sample capacitance while a ratio in the order of several hundreds is preferred. Their model that depolarisation field has its origin in the field produced by a charged external capacitor is crucially dependent on this choice of low standard capacitance.

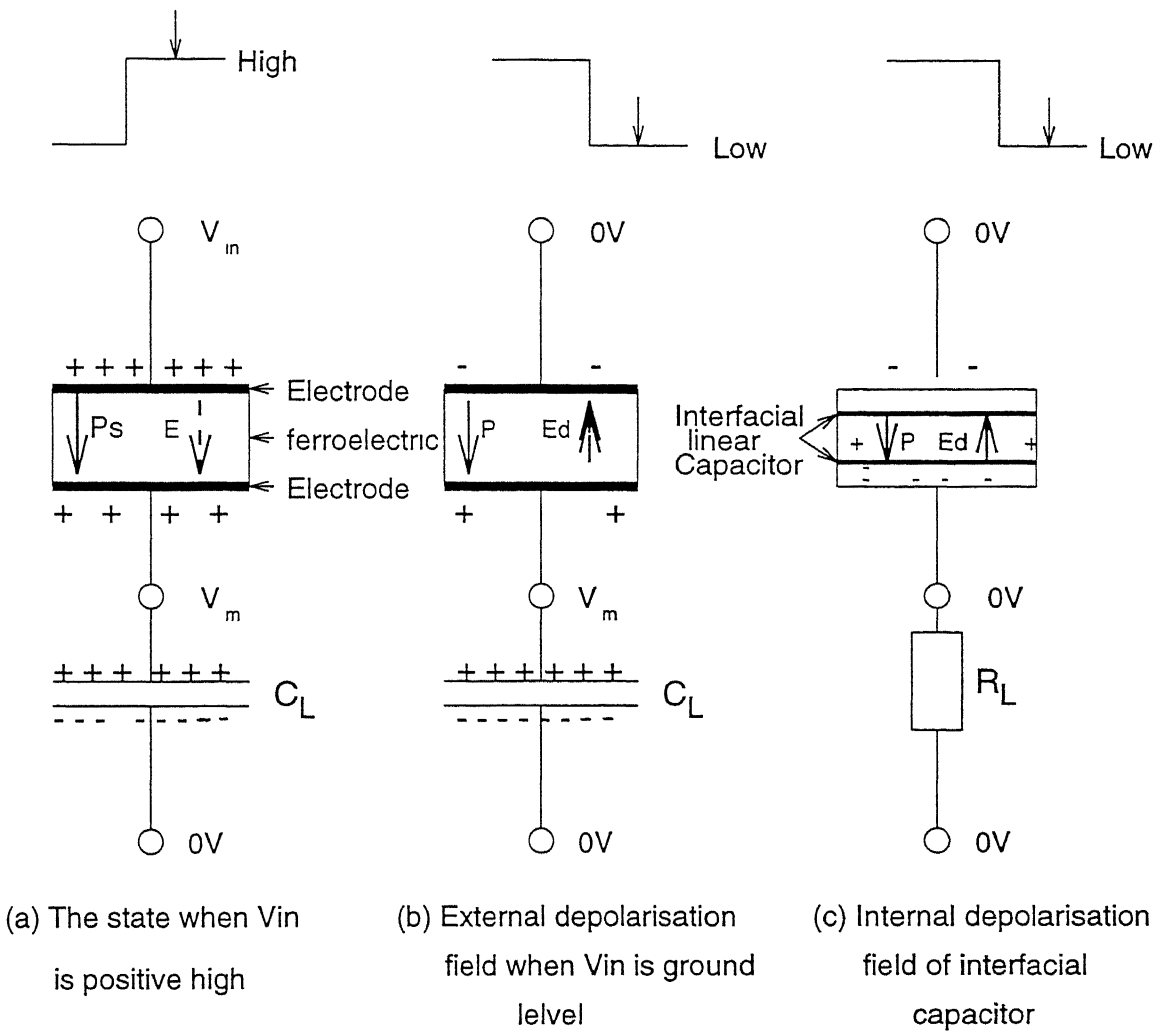


Fig. 1.4 Schematic of the Model For Generation of Depolarisation Field Proposed By Mihara et al

1.7 Definition of the Problem

It is evident from the preceding review that there is a lack of coherent understanding of depolarisation phenomenon in PZT thin film capacitors. In this work, we have adopted a new measurement sequence which enables us to monitor the phenomenon in the time domain after subjecting the sample to various combination of polarisation state sequence. We also relate it to other electrical parameters through Polarisation-electric field measurements at various steps of measurements. We report several new characteristic features, which can provide significant clues regarding the underlying mechanisms. We have used for this purpose sol-gel PZT films which are otherwise well characterized.

Samples prepared under two different heat treatment conditions are used for studying the depolarisation behaviour. The phenomenon is studied with respect to pulse height, pulse width and temperature. We propose a model to explain the origin of depolarisation behaviour on the basis of trapping and detrapping of charge carriers in space-charge region in the sample.

The organisation of thesis is as follows: Chapter 2 has the details of sample preparation and description of experimental set-up, Chapter 3 contains the details of measurements and results. The results are discussed and a new model is proposed in Chapter 4 and Chapter 5 is a brief summary of conclusions drawn and scope for future work in this field of research.

Chapter 2

Experimental Details

2.1 Introduction

A wide variety of preparation techniques have been employed to produce PZT thin films such as sputtering, sol-gel, chemical vapour deposition (CVD), electron beam evaporation and laser ablation[12, 13, 14, 15]. The choice of an appropriate preparation technique depends on the final application of these ferroelectric films. The requirements for use in the electronic applications such as memories, is very stringent and some of the major requirements are strict control of stoichiometry, uniform deposition over a large area (diameter around 100mm to 200mm), high deposition rate and high throughput. Among the techniques mentioned above, sol-gel process offers the advantages of molecular homogeneity, high deposition rate and high throughput and excellent composition control. In addition, the deposition can be under ambient conditions and it is easy to introduce dopants into the films. All the samples for the present work were prepared utilising the sol-gel method.

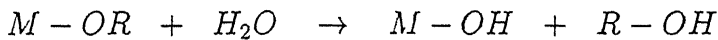
2.2 Sol-Gel Method

Sol-gel technology arose as a method of fabrication of high quality ceramics and glasses. The term sol represents the solution of sub-micron particles and gel represents the interconnected porous mass obtained from the sol. In the recent years, this technique has been extended to the fabrication of thin films or coatings of different substrates. In particular, attention has been given to the production of films of materials such as ferroelectric PZT, the high temperature super-conductor yttrium-barium copper oxide, conductive coatings of indium tin oxide and optical and protective coatings of complex oxides[16].

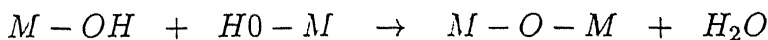
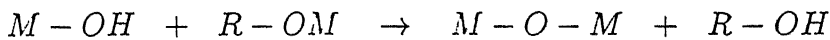
There are essentially, two different kinds of sol-gel technology. The first a colloidal method, involves the dispersion of colloidal particles in a liquid to form a sol and then destabilization of the sol to produce a gel. The second method involves the polymerization of organometallic compounds, such as alkoxides to produce a gel with a continuous network[17]. In the present work, the PZT thin films were prepared using the second method.

In the present context, the term sol-gel is used to describe chemical processes in which the polymeric gels are formed from metallo-organic starting solutions. The most commonly studied sol-gel systems are based on the chemistry of the metal alkoxides $M(OR)_n$. Many of these species readily undergo hydrolysis and condensation reactions, leading to oligomer formation and eventual gelation. The key steps in the gel forming reactions can be summarized as follows:

HYDROLYSIS



CONDENSATION



For thin film work, the gel forming solutions are coated onto suitable substrates by spin-on, dip or spray coating techniques, after which drying and firing stages convert the gel coating to an oxide film. In the present study, PZT thin films were prepared by spin coating technique.

In sol-gel processing, chemicals for preparing films are dissolved in a liquid to form a solution. Since all the starting materials are mixed at the molecular level in the solution a high degree of homogeneity of film can be expected. Another advantage of the sol-gel process is that because of the solution form of raw materials, trace elements can be easily introduced into the solution by adding the elements in the form of organo-metallic compounds or soluble organic or inorganic salts. Such trace elements can be important in adjusting the microstructure or in improving the properties of the oxide films[18]

2.3 Preparation of $Pb(Zr_{0.53}Ti_{0.47})O_3$ Thin Films

The PZT ceramics are chemically represented by $Pb(Zr_xTi_{1-x})O_3$. They are perovskite solid solutions and can exist in any one of the three crystal structures: tetragonal, rhombohedral and orthorhombic. The boundary between tetragonal and rhombohedral phases at $x = 0.535$ is a sharp morphotropic phase boundary (MPB). The compositions in the MPB region are of great technological interest because of high values of piezoelectric coefficients, large remanent polarization, reasonable coercive field etc., Hence, for the present work samples with morphotropic composition ($x = 0.535$) have been prepared.

Precursor solution for the preparation of films are prepared utilising modified sol-gel process proposed by Desu et al[15]. The starting materials for the preparation

Table 2.1
Chemicals used in Preparing the Sol

| S.No. | CHEMICALS | MOLES |
|-------|-----------------------|-------|
| 1. | Lead acetate | 1.05 |
| 2. | Acetic acid | 6.60 |
| 3. | Zirconium-n-Propoxide | 0.53 |
| 4. | Titanium-4-butoxide | 0.47 |

of the sol are lead acetate, zirconium-n-propoxide, titanium-4-butoxide and acetic acid. The acetic acid is used as a chelating agent to increase the shelf life of the precursor solution. To prepare the film a small amount of stock solution was taken and calculated amount of propanol and acetic acid were added to it. The relative amounts of various chemicals used in a typical sol are given in Table 2.1.

A 5 mole% of excess lead was used to compensate for any lead loss during the heat treatment cycle.

Platinum substrates have been used in this work as it is convenient for electrical contact and also it is known that high quality PZT films are obtained on it. Prior to the film coating, the platinum substrates are polished mechanically using velvete cloth and $1\mu\text{m}$ Al_2O_3 particles dispersed in water. The polishing is continued till a mirror finish is obtained. The polishing is done to remove any pinholes, surface imperfections which may lead to poor quality of films. The substrates were then

cleaned using the cleaning procedure as shown in Fig. 2.1.

By this cleaning procedure, thin layer of oxide and other impurities are removed

2.3.1 Spin Coating

The PZT thin films for the present work are prepared using the spin coating technique. The platinum substrate is fixed on the head of a centrifuge (REMI INSTRUMENTS) and rotated at 5000 R.P.M. The precursor solution is applied to the substrate using a syringe and after coating, the substrate is rotated for 5sec to obtain uniform film thickness which is inferred by observing the interference colours of the film. The film thickness formed in a single coating is mainly controlled by the viscosity of the solution and spin speed (in R.P.M). The viscosity of the solution is directly related to the molar concentration of the solution[19]. The film thickness linearly increases in proportion to the increase in molar concentration of the solution. Empirically, film cracking is directly related to the film thickness as well as the heating rate. Film cracking occurs when the thickness in a single coating is larger than a critical value. For PZT films on the platinum substrates, the tendency for the film cracking increases sharply, when the molar concentration of the PZT solution is larger than 0.5M. Therefore, the molar concentration of the solutions used in this work are kept less than 0.5M.

The film thickness can also be controlled by the spin speed. The relationship is given by equation[15]

$$t = k\omega^n \quad (2.1)$$

where, t = film thickness

k = constant dependent on evaporation rate, viscosity, the diffusivity and molecular weight of the solvent,

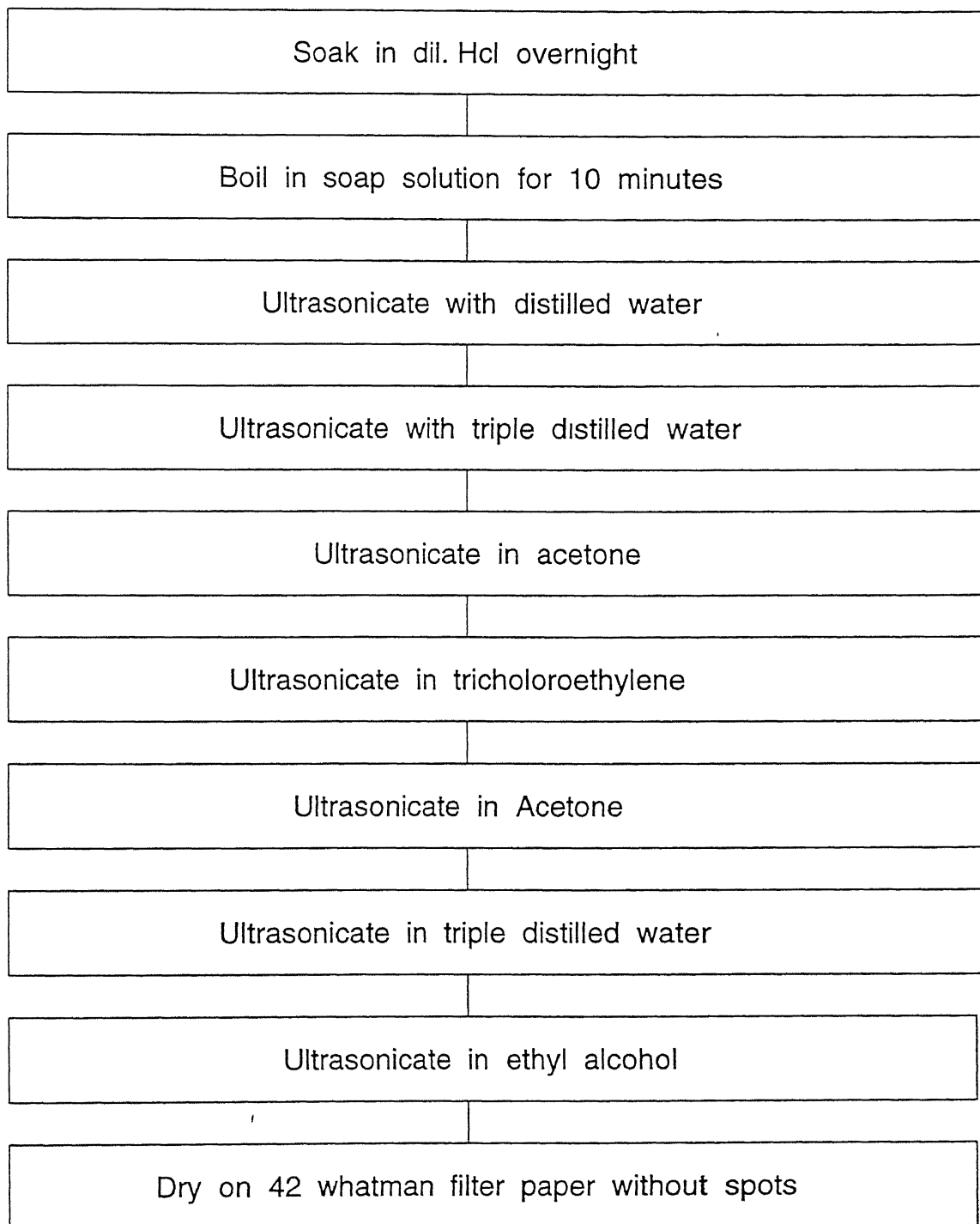


Fig. 2.1 Block diagram for substrate cleaning procedure

ω = spin speed, and

n = - 0.5

2.3.2 Firing and Annealing

Two types of firing and annealing as proposed by Majumder et al[20] was used in this work. After each coating, the film was fired at 400° C for 30minutes to drive off the organics present in the film. The film thickness can be increased by repeating the spin coating - firing sequence. After required thickness is obtained, the film was annealed at 700° C for one hour to obtain the crystalline film. The film obtained by this heat treatment is termed here as the slow fired sample.

In the second case, after each coating the film was fired at 600° C for 30 minutes to drive off the organics. The spin coating-firing sequence was repeated to obtain the desired film thickness. After this, film was directly introduced into the furnace at 700°C and annealed for one hour. The film obtained by this method is termed here as the fast fired sample. In both the slow and fast fired samples firing and annealing was done in O_2 ambient, to maintain the stoichiometry of the solution. The schematic of the heat treatment adopted for slow fired films is given in Fig. 2.2 and for Fast fired films is given in Fig. 2.3.

The flow diagram of the preparation of PZT films using the modified sol-gel process is as given in Fig. 2.4.

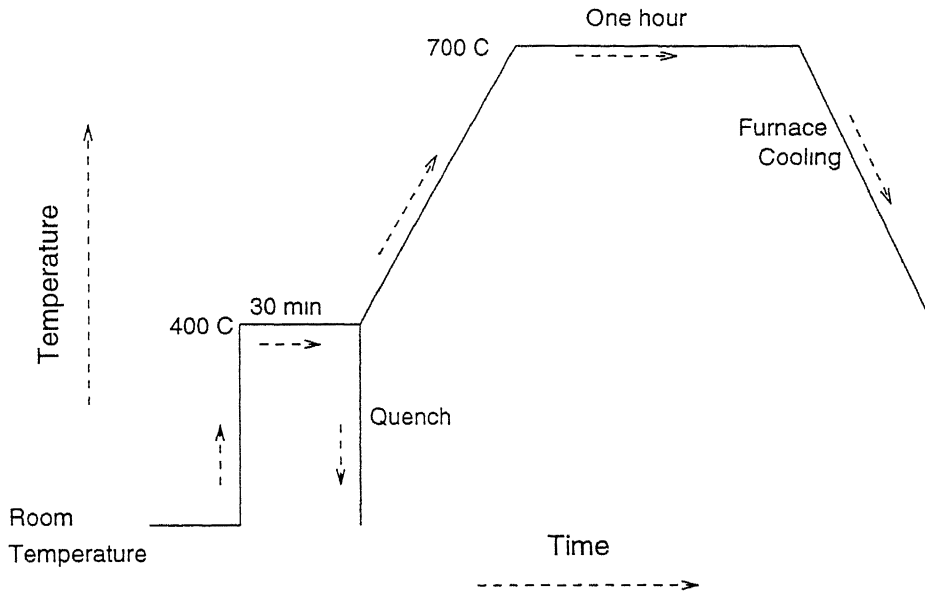


Fig. 2.2 Heat treatment for slow fired sample

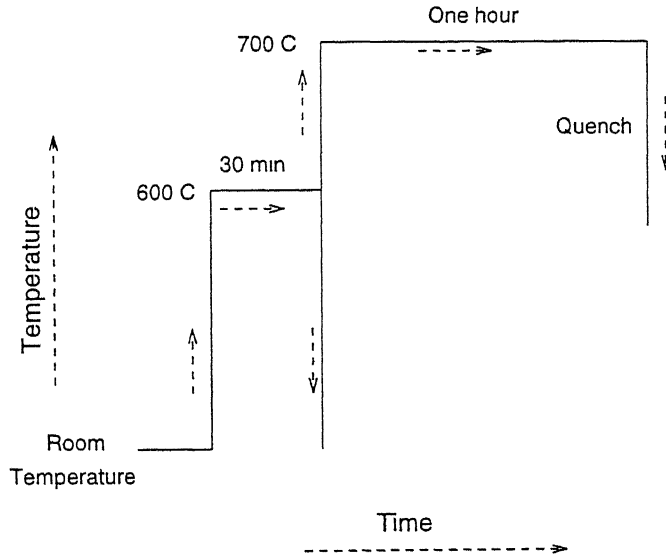


Fig. 2.3 Heat treatment for fast fired sample

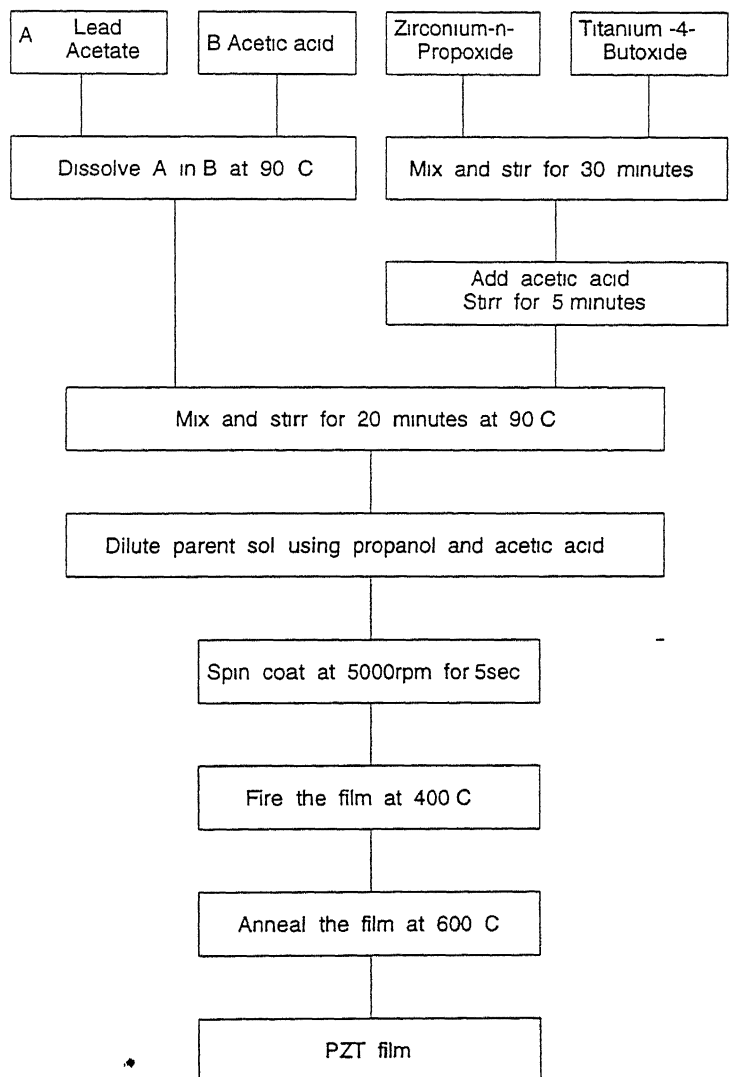


Fig 2.4 Flow diagram for preparation of PZT thin films

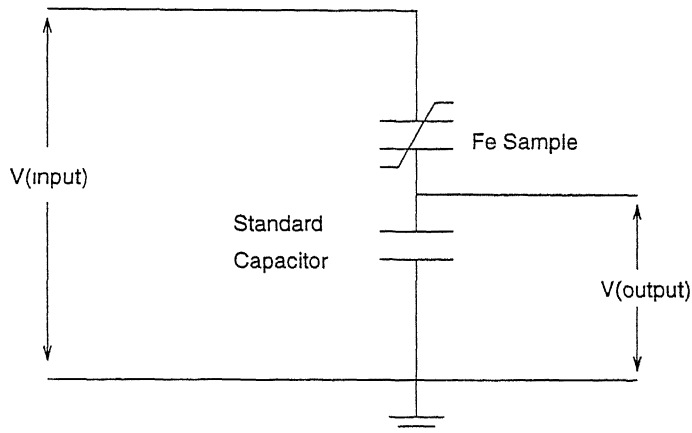


Fig. 2.5 Schematic of modified Sawyer-Tower circuit

2.4 Experimental Details

2.4.1 Experimental Set-Up For Hysteresis Measurements

The hysteresis measurements were carried out using the conventional Sawyer-Tower circuit[11]. The Schmeatic of Sawyer-Tower circuit and it's implementation are given in Figs. 2.5 & 2.6. By measuring the voltage acorss the standard capacitor, the polarization value of the sample can be determined. A bipolar triangular voltage of desired peak voltage is generated at 0.4Hz using the computer. The voltage is then amplified by the bipolar voltage amplifier (KEPCO BOP1000M). The amplified voltage is then applied across the sample-standard capacitor combination. The standard capacitance is usually very large compared to the sample capacitance so that most of the applied voltage drops across the sample.

The voltage across the standard capacitor is measured using the electrometer (KEITHLEY 610C) which has very high input impedance ($10^{14}\Omega$). The value of the standard capacitor used in our work is 225nF. The output of the electrometer is

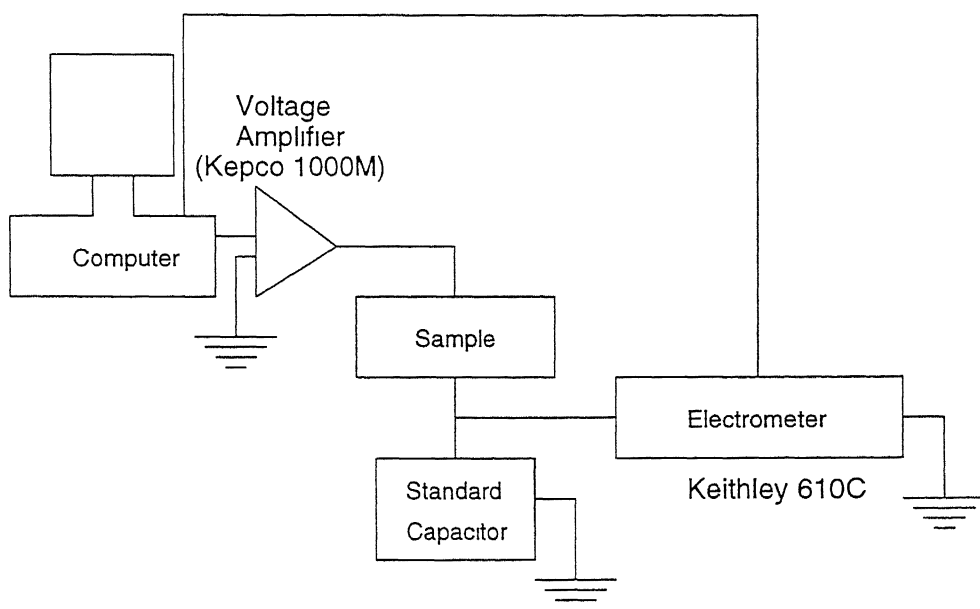


Fig. 2.6 Schematic of implementation of modified Sawyer-Tower circuit

read back using the AD card and the readings are stored in a data file. The sample polarization is calculated according to the following equation

$$P = Q/A$$

$$\text{Or } P = C V_{out}/A$$

where, P = sample polarization. C = capacitance of the standard capacitor, V_{out} = voltage across the standard capacitor, and A = area of the sample capacitor

2.4.2 Description of Set-up For Depolarization Measurements

The depolarization measurements were also carried out using the conventional Sawyer-Tower circuit. A square voltage pulse of desired magnitude is generated using an

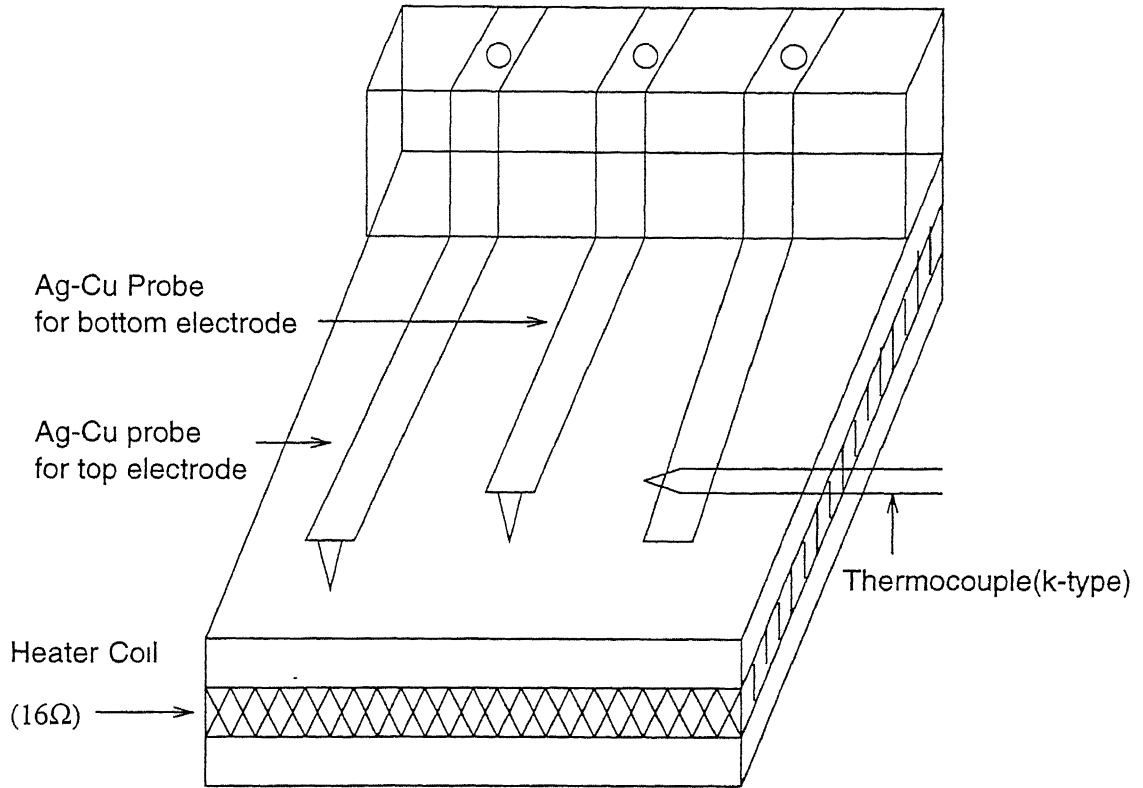


Fig. 2.7 Sample holder for P-E measurements

D/A add-on card in the computer. The voltage pulse after amplification using the bipolar voltage amplifier (KEPCO BOP1000M) is applied across the sample-standard capacitor combination. By measuring the voltage across the standard capacitor, the polarization of the sample is calculated. The polarization is monitored as a function of time. To enable recording of long transients, the sampling time interval between the data points is chosen to be different for each decade of time.

2.4.3 Description Of The Sample Holder

The sample holder used in the hysteresis measurements is shown in the Fig. 2.7. It

has been made using the Ag-Cu alloy. The probes used in it for making electrical contacts to the sample, are mounted on the base using a teflon block. The sample holder has an additional arrangement for temperature measurement. For heating the sample to desired temperature, it has been equipped with 16Ω heater coil.

A sample holder was constructed, which can be used for performing the Hysteresis loop measurements, Capacitance-Voltage and electron emission experiments. The base of the sample holder, supporting platforms for the grids and the holder for the collecting electrode were made of perspex. The distance between the grids and the sample can be varied. The arrangement for this variation is made by making slots in the aluminium blocks and sliding the grids and collecting electrode through it as shown in the Fig. 2.8. The electron emission experiments can be done without the grids also by removing them from the set up. The collecting electrode can be held as close as possible (3mm) to the sample. The electrical connections to the bottom electrode is made through an aluminium foil fixed on the top of the bottom platform. The electrical connections to the top electrodes is made through either using a probe made up of spring steel or using thin copper wires connected to the electrodes using the silver paste. The collecting electrode or anode is an ITO (Indium tin oxide) coated glass which can be maintained at any desired potential with respect to the sample. The experiments can be done with one or two grids. The One of the grid can be used in the grounded configuration to reduce the the electromagnetic noise. The other grid can be maintained at same potential as the collecting electrode for accerlating the electrons emitted from the ferroelectric sample. The whole assembly is maintained inside a vaccum chamber during measurements. The vaccum chamber is evacuated using the Rotary pump. However, electron emission measurements were not carried out in this work. The present sample holder is convenient for many planned experiments related to this work.

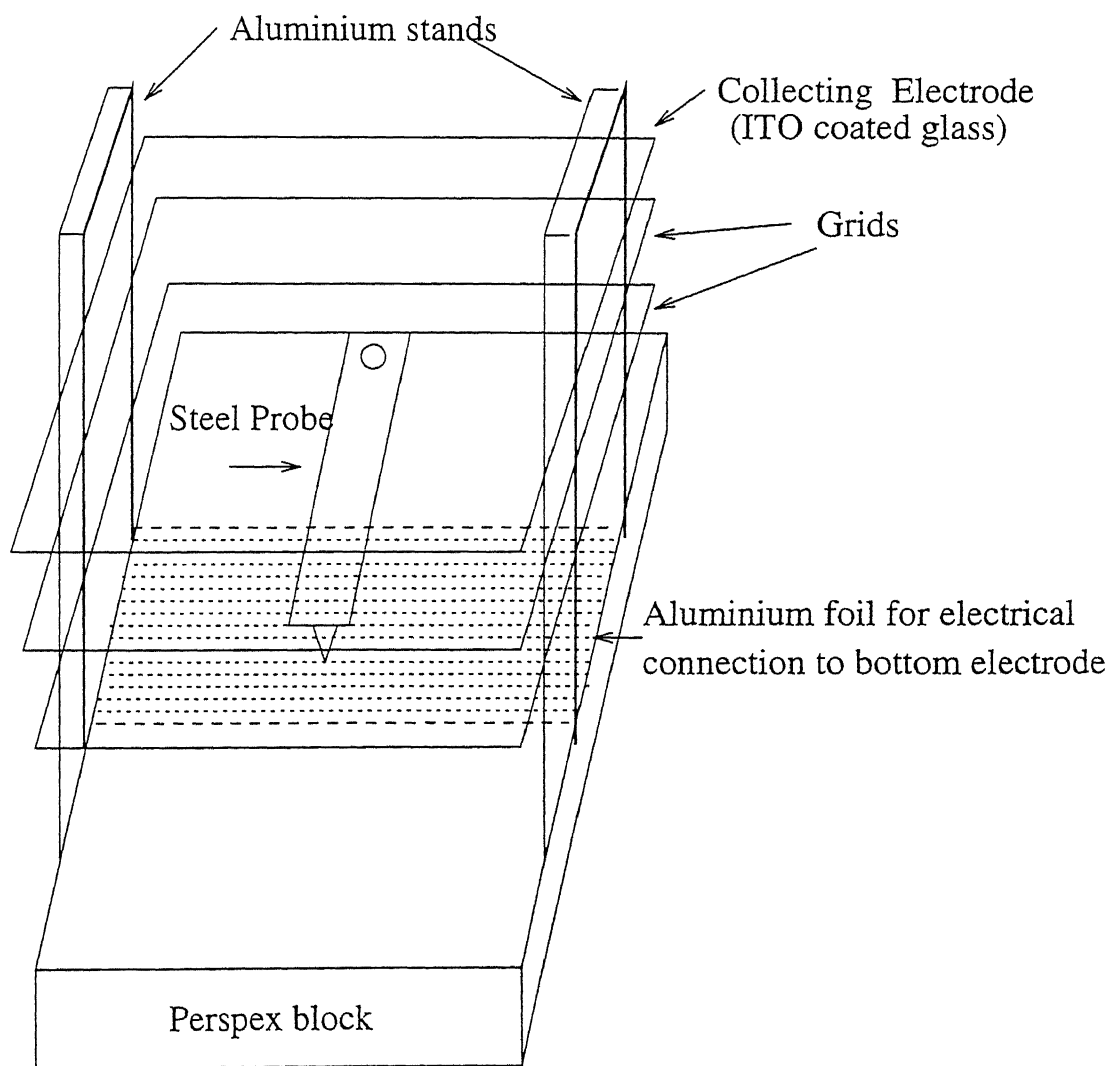


Fig. 2.8 Schematic of the Sample Holder Used in the Electron Emission Experiment

Chapter 3

Measurements and Results

In this chapter, we present the measurements and results, leaving their discussion to the next chapter.

3.1 Sample Details and Standard Characterization

The $Pb_{1.05}(Zr_{0.53}Ti_{0.47})O_3$ thin films used in this work are prepared by sol-gel method. For studying the depolarisation characteristics, samples prepared with two different heat treatment sequences are used. The sample which is fired at 400°C and annealed at 700°C is mentioned as slow fired sample. The sample which is fired at 600°C and annealed at 700°C is mentioned as fast fired sample.

The thickness of the films used in this work are measured using the surface profilometer (Model alpha step100.Tencor instruments). The thickness of the slow fired sample is $1.25\mu m$ and that of the fast fired sample is $0.8\mu m$.

The phases in the film are determined by X-ray diffractometer (Richseifert Iso debyeflex-2002), using $Cu - K\alpha$ radiation with a monochromator. The formation

of perovskite phase in the both fast and slow fired samples (cf. §2.5) is confirmed by analysing the X-ray diffraction pattern. The quality of the samples used in this work are at par with the samples reported in the literature and this has been confirmed by various studies on phase formation, microstructure and electrical characterization of the samples by Majumder et al[20], in our laboratory.

For evaluating the depolarisation characteristics of the samples, circular Au-Pd electrodes of diameter 0.6mm and 0.5mm are deposited on the fast and slow fired samples respectively. The electrodes are deposited using the sputtering unit (Hummer VA-Anatech Ltd.,) operating at 80 mtorr in argon ambient.

3.2 Polarisation - Electric Field Measurement

The polarisation of the sample as a function of the applied electric field is studied using an automated modified Sawyer-Tower circuit[11]. P-E loop exhibits expected non-linear dielectric behaviour, i.e., hysteresis which separates ferroelectrics from linear dielectrics. The hysteresis behaviour is because of the spontaneous polarisation at temperatures less than the Curie temperature. At lower field strengths in unpolarised material the polarisation is initially reversible and is nearly linear with the applied electric field. At higher field strengths, the polarisation increases considerably as a result of switching of the ferroelectric domains. At higher field strengths, the change in polarisation is small due to polarisation saturation. In this condition, all the domains of like orientation are aligned with the field. Extrapolation of the high field polarisation back to zero gives the spontaneous polarisation (P_s). When the applied field continues to be applied at values greater than required to achieve P_s , the spontaneous polarisation continues to increase but only proportional to initial dielectric constant. When electric field applied to sample is cut off,

the polarisation does not go to zero but remains at a finite value called remanent polarisation(P_r). This is due to oriented domains being unable to return to their random state without an additional energy input by an oppositely directed electric field. The strength of the electric field required to make the polarisation (P) of the sample to zero is called coercive field(E_c)

Typical hysteresis loops for slow and fast fired samples are given in Figs. 3.1–3.2. The remanent polarisation (P_r) of the slow fired and fast fired sample are nearly

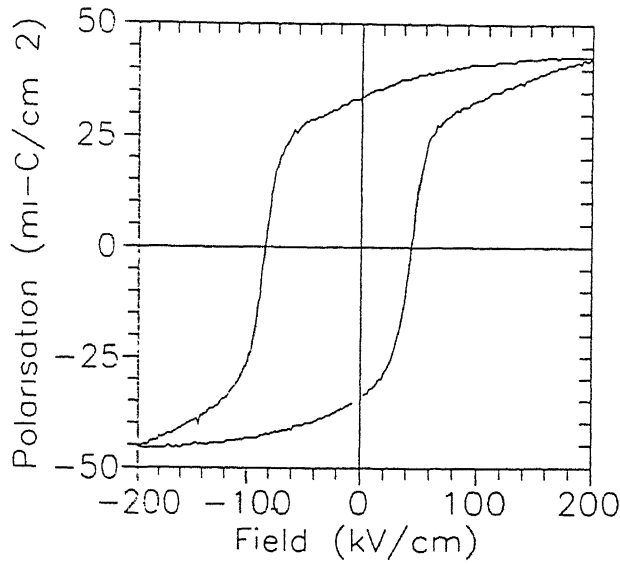


Fig 3.1 P–E characteristics of slow fired sample

same ($35\mu C/cm^2$). The coercive field E_c for the slow fired sample is 64 kV/cm which is less than the E_c of fast fired sample (84 kV/cm).

The P–E measurements which are carried out on the freshly prepared sample capacitors exhibited asymmetry along the polarisation and field axis. This asymmetry is not a pronounced one. When the P–E measurements are carried for the second time on these fresh capacitors, the hysteresis loops are shifted along the polarisation

axis but the asymmetry along the field axis is maintained. The shift along the polarisation axis (Y-axis) is merely due to the initial potential of the standard capacitor and only need to be subtracted to obtain the true hysteresis loops. However, the asymmetry along field axis (X-axis) has more fundamental physical origin.

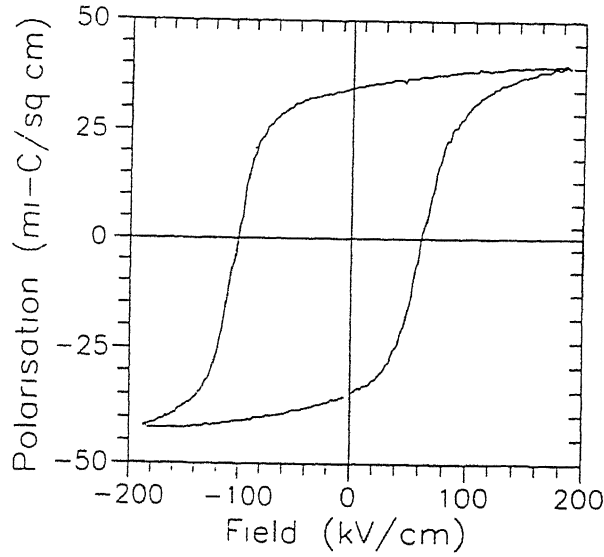


Fig 3.2 P-E characteristics of Fast fired sample

Nearly all the P-E measurements carried out in this work, resulted in hysteresis loops exhibiting asymmetry along the field axis. An asymmetry is expected along the field axis only when a dc bias is superimposed on the measuring ac field. But, in our measurements there is no such superimposition and it appears as if there is dc bias naturally existing inside the sample. This bias is called the internal bias and it is calculated from the asymmetry of hysteresis loops along the field axis as

$$E_i = \frac{E_{c+} - E_{c-}}{2} \quad (3.1)$$

Where E_i = Field due to internal bias, E_{c+} = value of coercive field along the positive field axis, and E_{c-} = value of coercive field along the negative field axis.

Hence, the sign of E_i (which determines the orientation of E_i inside the sample) is positive if loop is shifted along the positive field axis and it will be negative, if it is shifted along the negative field axis. Throughout the course of this work, hysteresis loops for many samples under different conditions have been studied. We found a relation between the asymmetry and sign of saturation polarisation exhibited in all these loops. For example, in Fig. 3.3 the loop is shifted along negative field side and the saturation of polarisation is well pronounced in positive field side. In Fig.

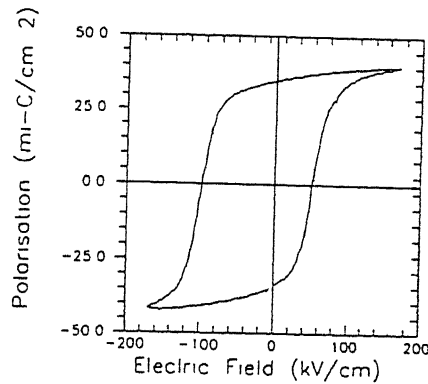


Fig. 3.3 P-E Loop Showing Relation Between Field Asymmetry With Polarisation

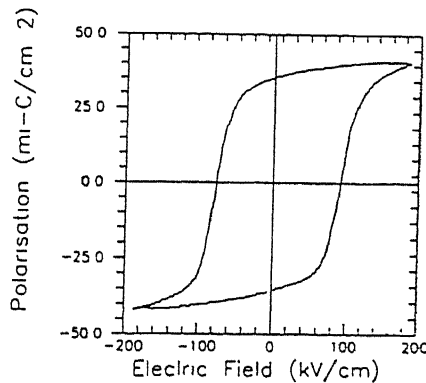


Fig. 3.4 P-E Loop Showing Relation Between Field Asymmetry With Polarisation

3.4, the loop is shifted along the positive field side and saturation of polarisation is well pronounced in the negative field side. This relation is due to the presence of internal bias inside the sample. We will present more results on the internal bias in the following sections

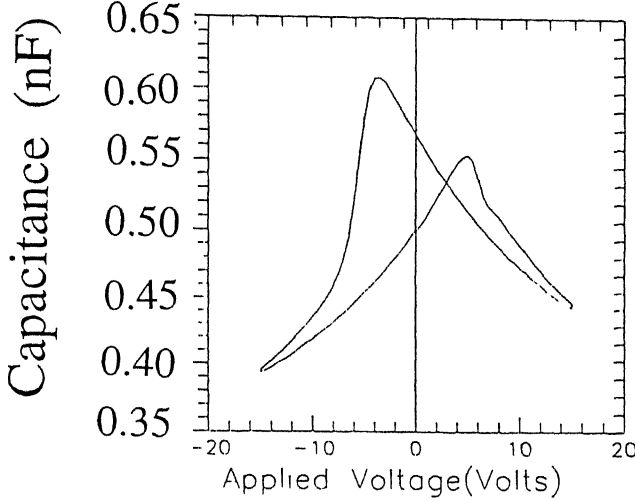


Fig. 3.5 C-V Loop Exhibiting Asymmetry Along Voltage and Capacitance axis

3.3 Capacitance – Voltage Measurements

The small signal capacitance of the sample is measured using the Impedance analyser (HP 4192A). For this measurement a dc field is swept from $-V_{max}$ to $+V_{max}$ in steps of 0.5V increments with a step rate of 1step/sec. The sweep of the dc field modulates the polarisation state of the sample across the P-E hysteresis loop. Thus, the capacitance changes with the d.c field as (dielectric constant $\propto dP/dE$) resulting in hysteric C- V loop rotating in direction. The variation in the dielectric response

with the dc field is associated with domain switching process[21]. For low dc fields, the main contribution to the dielectric constant is the increase in polarisation due to domain reversal. The fields corresponding to the dielectric constant maxima are approximately equal to the coercive fields determined from the P-E hysteresis loops. For high dc fields most switchable domains align along the direction of the electric field. The dielectric constant is relatively small since it is mainly determined by the vibrations of the dipoles. Therefore the shape of the C-V loop contains information regarding distribution of relaxation times of domains. The C-V characteristics of fast fired sample studied at 100kHz is given in Fig 3.5. From the zero bias values of the capacitance, the dielectric constant of the samples are determined. The dielectric constant of the slow fired sample and fast fired sample is nearly same (313 and 323 respectively in this case).

The C-V loops recored on the samples also exhibited asymmetry along the voltage and capacitance axis. The asymmetry of the C-V loops along the voltage axis is due to presence of internal bias. Here also there exists a definite relation between the asymmetry along the voltage and capacitance axis. If the loop is shifted along the positive voltage side then the peak value of capacitance in the negative voltage side is larger than in the positive voltage side. This relation is another manifestation of the relation between polarisation state and E_i found through P-E measurements.

3.4 Depolarisation measurements

3.4.1 Description of the Measurement Sequence

As mentioned in Chapter 1, various fast pulse sequences have been used in the literature to study depolarisation characteristics of the ferroelectric lead zirconate titanate thin films.

Benedetto et al studied depolarisation characteristics with respect to magnitude of the applied voltage pulse and temperature. The fatigue dependence was also studied. Mihara et al carried out an extensive study of the depolarisation characteristics of PZT with respect to number of measurements, width and height of applied voltage pulse, excess Pb %, temperature dependence and the dependence on the load capacitance. However the time dependence of the polarisation was not carried out by Mihara et al.

Further in their measurement sequence, P-E measurement was not included. Hence any possible changes in the sample parameters like P_r , E_c etc., due to depolarisation measurements was not detected.

We adopted a new measurement sequence for evaluating the depolarisation characteristics of the ferroelectric lead zirconate titanate thin films, which includes P-E measurements and explicit observation of depolarisation characteristics in the time domain. The steps adopted for evaluation of depolarisation characteristics are given below.

1. Polarise the sample to the particular polarisation state using P-E measurements. Usually, P-E measurements leave the sample in a definite polarisation state and hence by changing the voltage sequence applied to the sample during the P-E measurements, the desired polarisation state ($+P_r$ or $-P_r$) can be achieved.
2. Polarisation of the sample is switched (non-switched) by applying a square voltage pulse. The magnitude of the pulse is equal to the voltage at which polarisation of the sample saturates. The width of the voltage pulse can be varied. Once the voltage pulse is applied to the previously polarised sample, the corresponding change in polarisation values are monitored as a function of time. The time scale starts when the voltage pulse is applied to the sample. The typical monitoring time for depolarisation measurements is one hour.

Table 3.1

| Initial Polarisation state | Polarity of applied Voltage pulse * | Final Polarisation state | Mentioned as (S.C : switching case N.S.C : Non-switching case) |
|----------------------------|-------------------------------------|--------------------------|--|
| +Pr | Negative | -Pr | +Pr : S.C |
| +Pr | Positive | +Pr | +Pr : N.S.C |
| -Pr | Positive | +Pr | -Pr : S.C |
| -Pr | Negative | -Pr | -Pr : N.S.C |

* Polarity of the applied voltage is determined w.r.t top electrode of the sample. If the top electrode is at higher potential than bottom electrode, then the applied voltage is positive and vice versa

3 After the depolarisation measurements are over, P-E (Polarisation Vs Electric field) measurements are again carried out on the sample, to monitor any changes during the course of depolarisation.

In step-2, depending upon the polarity of the applied voltage, we will have either switching or non-switching of the previously polarised state. Since the initial polarisation state of the sample can be either $+P_r$ or $-P_r$, we will have four different cases, depending upon the initial polarisation state and polarity of the applied square voltage pulse. The different combinations are summarised in Table 3.1.

The depolarisation characteristics of the ferroelectric lead zirconate titanate thin films are studied with respect to the following parameters:

1. Magnitude of the applied voltage pulse

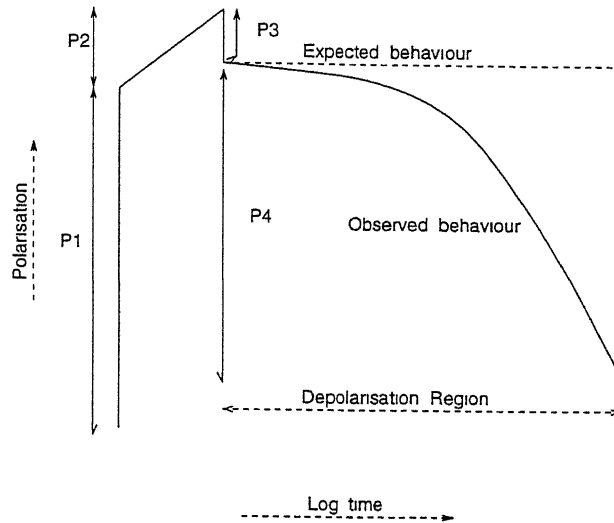


Fig 3.6 General features of depolarisation characteristics of Ferroelectric lead zirconate titanate

2. Width of the applied voltage pulse
3. Temperature

3.4.2 Description of the General Behaviour of the Depolarisation Characteristics

The depolarisation characteristics of the lead zirconate titanate thin films in general, consists of four different regions. The schematic of the four different regions of depolarisation characteristics is given in Fig. 3.6.

When a square voltage pulse is applied to the previously polarised sample, there is an instantaneous rise of polarisation. The magnitude of rise in the switching cases is larger than the non-switching cases. The amount of instantaneous rise of polarisation is represented by P1. This instantaneous rise of polarisation is due to the nanosecond switching of polarisation. In the time interval during which the voltage

of the applied pulse remains constant i.e., width of the voltage pulse, there is a comparatively small increase in polarisation. The amount of increase of polarisation in this second region of the depolarisation characteristics is represented as P2. The rise in this region is due to leakage current of the sample, which gets integrated by the standard capacitor used in the depolarisation measurements.

When the applied voltage pulse becomes zero, there is an instantaneous loss of polarisation. The amount of loss of polarisation in this third region of depolarisation characteristics is given by P3. The loss of polarisation in this region is due to the reverse nucleation of the domains, before applied field value become equal to the coercive field.

Ideally, the zero field value of the polarisation i.e remanent polarisation should be maintained by the ferroelectric sample for long time. But in the measurements it is observed that polarisation starts to decay from this zero field value. This fourth region of the depolarisation characteristics is of our interest and this region is called as the depolarisation region and amount of loss of polarisation in this region is given by P4.

In different cases of switching and non-switching of polarisation, the loss of polarisation is different. In order to get a generalised picture of this loss, the polarisation loss at the end of fixed amount of time is given in terms of percentage which is calculated as given below:

$$\text{Polarisation loss} = (P4/P_r) \times 100\%$$

where $P4$ = Amount of loss of polarisation in the depolarisation region, and P_r = Remanent polarisation of the sample.

For analysing the decay transient, we have used the technique of time analysed transient spectroscopy (TATS). In this technique a signal $S(t)$ is constructed from the depolarisation curve as

$$S(t) = P(t_1) - P(t_2) \quad (3.2)$$

For a decaying curve, this signal would go through a maximum at a certain time $t(\max)$. For specificity, if we assume that the decaying signal is an exponential with a time constant (τ) , then

$$S(t) = P_0[e^{-t_1/\tau} - e^{-t_2/\tau}] \quad (3.3)$$

where P_0 is the total strength of the exponential or $P_0 = P(0) - P(\text{infinity})$. For this case $t(\max)$ and τ are related as

$$\tau = t(\max)/\ln 2$$

The signal also provides a measure of non-exponentiality if any, through the comparison of the line shape. The other advantage is that the presence of constant value gets automatically eliminated from the analysis. It is enough to obtain a peak to be able to calculate the time constant. Hence, the time constant can be calculated, even when the saturation of polarisation is not observed. The schematic of the result of analysis of an exponential decay of polarisation with TATS is given in Fig. 3.7.

The sample parameters P_r , E_c and E_i are noted down before and after the depolarisation measurements. There is no change in values of P_r and E_c of the samples after the measurements. This implies that loss of polarisation is not due to any degradation of the sample, as it is observed in fatigue.

In all our depolarisation measurements with four different cases of switching and non-switching of polarisation and with respect to all adopted experimental parameters, there exists a strong relation between the polarisation state achieved in the depolarisation measurements by applying a square voltage pulse, with the orientation of final E_i . If the achieved polarisation state is $-P_r$, then the final E_i is found to be positive in sign(oriented downward inside the sample according to our

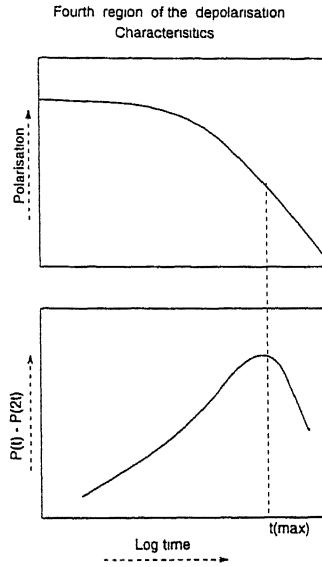


Fig 3.7 Schematic of $P(t)-P(2t)$ Plot

convention) and if the achieved state is $+P_r$, then the final E_i is negative (oriented upward inside the sample).

The results of the depolarisation measurements are given in the form of tables which contain the following parameters:

1. Initial rise of polarisation given by $P_1(\text{in } \mu\text{C}/\text{cm}^2)$
2. Rise of polarisation in the second region given by $P_2(\text{in } \mu\text{C}/\text{cm}^2)$
3. Loss of polarisation in the third region given by $P_3(\text{in } \mu\text{C}/\text{cm}^2)$
4. Loss of polarisation in the depolarisation region given by $P_4(\text{in } \mu\text{C}/\text{cm}^2)$
5. Polarisation loss in percentage (compared with remanent polarisation P_r)
6. Initial value of internal bias E_i (in kV/cm)
7. Final value of internal bias E_i (in kV/cm)
8. Time constant of the decay of polarisation (in sec)

The coercive field value E_c is not tabulated because this parameter is not affected by the depolarisation measurements. In some cases the time constant of the decay

process is not tabulated because of the fact that decay process is very slow in these cases

3.5 Depolarisation Measurements on the Fast Fired Sample

The depolarisation behaviour of the fast fired sample is studied with respect to adopted experimental parameters like pulse height, pulse width and temperature.

3.5.1 Dependence of the Depolarisation Characteristics on the Magnitude of the Applied Voltage Pulse

For this study, depolarisation measurements are carried out on the fast fired sample (mentioned hereafter as capacitor-1). Two different magnitudes of switching voltage 15V and 20V are chosen and width of pulse in both these cases is 3.25s. The monitoring time for polarisation in the depolarisation measurements is one hour. The depolarisation behaviour in four different cases of switching and non-switching of polarisation are given in Figs. 3.8–3.11. The loss of polarisation is observed in all four cases. The loss of polarisation in $-P_r : N.S.C.$ and $+P_r : N.S.C.$ is small compared to the switching cases. In all the four cases, the rate of loss of polarisation is slow and hence the time constant is not calculated for the decay process. In the $-P_r : N.S.C.$ towards the end of measurement time, there is a slight increase of polarisation. But, this is due to small fluctuations in the values of polarisation while the decay is taking place. The results of the measurement is given in Table 3.2.

In the depolarisation measurements with pulse height being 20V, the general

Table 3. 2
Fast fired sample Capacitor-1
Applied voltage = 15V Polansation monitoring time = 3600sec

| Polarsation state | Switching case | Non-Switching case |
|-------------------|---|--|
| +Pr | <p>P1 = 69 P2=0.77 P3 = 8.54 P4 = 10.10</p> <p>Polarsation loss = 28.85 %</p> <p>Initial Ei = 22.5 kV/cm Final Ei = 4.63 kV/cm Time constant = ***</p> | <p>P1 = 12.43 P2 = 2.71 P3 = 6 P4 = 3.49</p> <p>Polarsation loss = 9%</p> <p>Initial Ei = 4.68 kV/cm Final Ei = -17.81 kV/cm Time constant = ***</p> |
| -Pr | <p>P1 = 76.15 P2 = 1.16 P3 = 7.38 P4 = 21.75</p> <p>Polarsation loss = 62.14%</p> <p>Intial Ei = -19.68 kV/cm Final Ei = -26.25 kV/cm Time constant = ***</p> | <p>P1 = 9.71 P2 = 3.10 P3 = 7.77 P4 = 1.94</p> <p>Polarsation loss = 5%</p> <p>Initial Ei = -26.25 kV/cm Final Ei = 6.56 kV/cm Time constant = ***</p> |

Table 3.3
Fast fired sample: Capacitor - 1
Applied Voltage = 20V Polarsation monitoring time = 3600sec

| Polarsation state | Switching case | Non-Switching case |
|-------------------|---|---|
| +Pr | <p>P1 = 67.99 P2 = 0.77 P3 = 9.32 P4 = 12.82</p> <p>Polarsation loss = 36.62%</p> <p>Initial Ei = 7.5 kV/cm Final Ei = 8.75 kV/cm Time constant = ***</p> | <p>P1 = 12.43 P2 = 2.33 P3 = 6.99 P4 = 7.38</p> <p>Polarsation loss = 21.08%</p> <p>Initial Ei = -13.75 kV/cm Final Ei = -23.12 kV/cm Time constant = ***</p> |
| -Pr | <p>P1 = 73.82 P2 = 1.94 P3 = 8.15 P4 = 21.37</p> <p>Polarsation loss = 61.05%</p> <p>Initial Ei = -15 kV/cm Final Ei = -21.18 kV/cm Time constant = ***</p> | <p>P1 = 8.57 P2 = 2.53 P3 = 8.15 P4 = 0.77</p> <p>Polarsation loss = 2%</p> <p>Initial Ei = -21.18 kV/cm Final Ei = 7.5 kV/cm Time constant = ***</p> |

features of depolarisation behaviour in all the four regions of depolarisation characteristics is similar to that of the corresponding cases in the 15V measurement i.e there is no remarkable change in the values of P1, P2, P3 and P4. Here also the decay of polarisation is found to be slow in all four cases of switching of polarisation. The results of the depolarisation measurements with pulse height of 20V are given

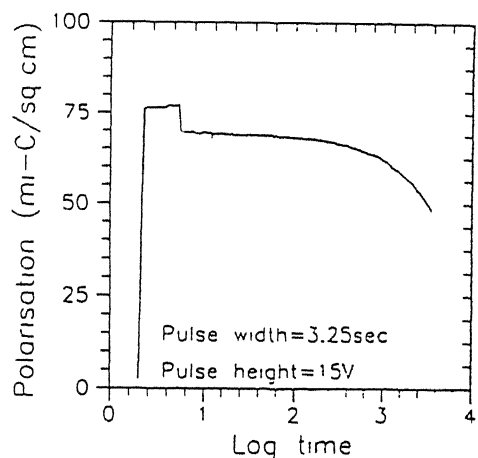


Fig 3.8 Depolarisation behaviour of -Pr:SC in Fast fired capacitor-1

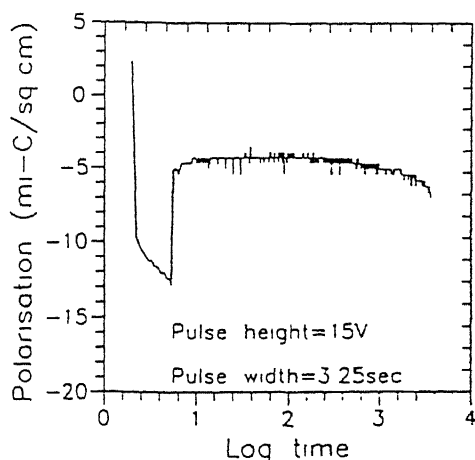


Fig 3.9 Depolarisation behaviour of -Pr:N.S.C in Fast fired capacitor-1

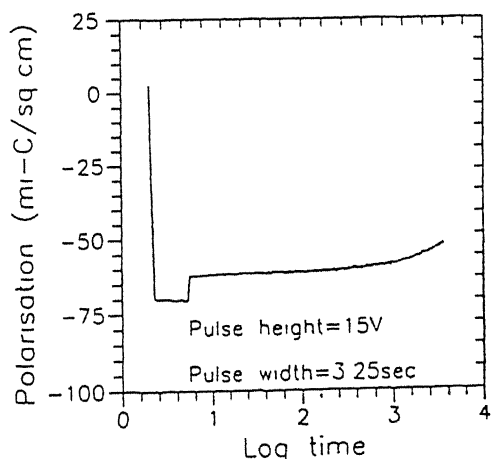


Fig 3.10 Depolarisation behaviour of +Pr:SC in Fast fired capacitor-1

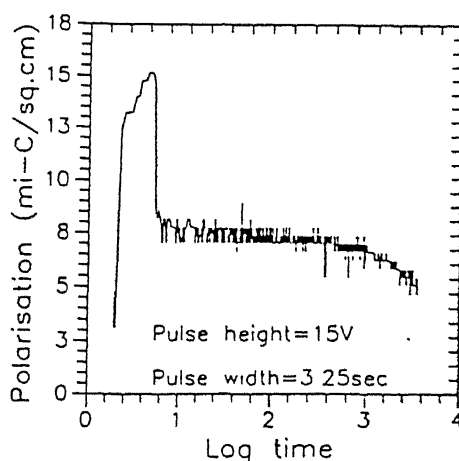


Fig 3.11 Depolarisation behaviour of +Pr:N.S.C in Fast fired capacitor-1

in Table 3.3. From, these results we can conclude that depolarisation behaviour is independent of the pulse height.

3.5.2 Dependence of Depolarisation on the Width of the Applied Voltage Pulse

For this measurement, a fresh capacitor from the fast fired sample is chosen (capacitor-2) In this measurement only particular case $-Pr:S C$ is chosen for the study. Magnitude of the applied voltage pulse is 15V and width of the applied voltage pulse are chosen to be 3.25s, 10.25s, 20.25s and 30.25s. The results of the measurements are given in Table 3.4 The changes in the values of polarisation in the four regions of depolarisation characteristics given by P1, P2, P3 and P4 are nearly of same magnitude for all pulse width adopted in this measurement. The rate of loss of po-

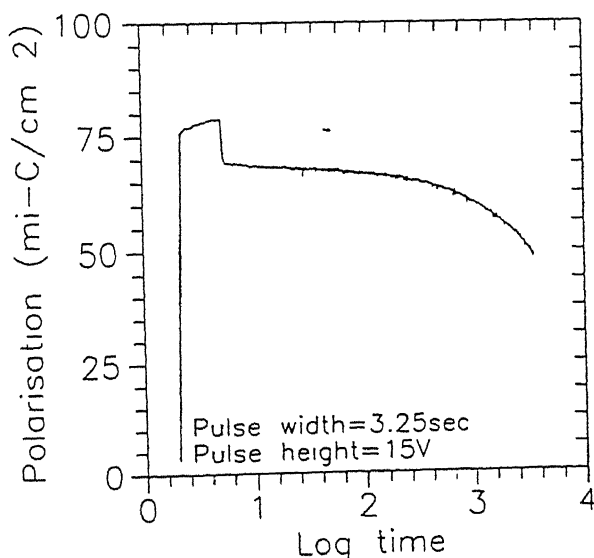


Fig.3.12 Depolarisation behaviour in $-Pr:S.C$ of Fast fired capacitor-2

Table 3 4
Dependence of depolarisation on the width of the applied voltage pulse
Pulse height = 15V
Fast fired sample capacitor-2 Polarsation monitoring time = 3600sec

| Width of applied voltage pulse | Case | Remarks |
|--------------------------------|---------|---|
| 3.25sec | -Pr S C | P1 = 75.76 P2 = 3.10 P3 = 8.54 P4 = 21.75 Polarsation loss = 65.90% Initial Ei = 15 kV/cm Final Ei = -21.56 kV/cm Time constant = *** |
| 10.25sec | -Pr S C | P1 = 73.43 P2 = 1.55 P3 = 6.99 P4 = 16.31 Polarsation loss = 49.42% Initial Ei = -22.5 kV/cm Final Ei = -24.37 kV/cm Time constant = *** |
| 20.25sec | -Pr S C | P1 = 75.76 P2 = 2.33 P3 = 7.77 P4 = 19.03 Polarsation loss = 57.66% Initial Ei = 13.12 kV/cm Final Ei = -18.75 kV/cm Time constant = *** |
| 30.25sec | -Pr S C | P1 = 74.21 P2 = 1.94 P3 = 6.99 P4 = 17.87 Polarsation loss = 54.15% Initial Ei = -18.75 kV/cm Final Ei = -22.5 kV/cm Time constant = *** |

larisation is slow in all four cases and hence the time constant of the decay process is not calculated. The depolarisation behaviour in the measurement with pulse width being 3.25s is given in Fig. 3.12. The depolarisation behaviour for the other pulse widths are similar to measurement with pulse width of 3.25s. The polarisation loss lies in this measurements lies between 50-65%. Even by increasing the pulse width to 30.25s, the depolarisation behaviour did not show any appreciable change. Hence, we conclude that depolarisation behaviour is independent of pulse width.

3.5.3 Back Switching and Decay Time Constant

In all the depolarisation results presented so far, the amount of polarisation loss in different cases showed sample to sample variation and percentage of polarisation loss

Table 3.5
Fast fired sample capacitor-3 Pulse height = 15 V
Width of the voltage pulse = 3.25 sec
Polarisation monitoring time = 3600 sec

| Case | Remarks |
|-----------|--|
| +Pr S C | P1 = 73.43 P2 = 6.99 P3 = 6.66 P4 = 48.57 Polarsation loss = 138% Initial Ei = -14 kV/cm Final Ei = 16.87 kV/cm Time constant = 975 sec |
| -Pr N S C | P1 = 5.05 P2 = 10.10 P3 = 5.43 P4 = 19.03 Polarsation loss = 54.37% Initial Ei = -13 kV/cm Final Ei = 15 kV/cm Time constant = *** |
| -Pr S C | P1 = 75.93 P2 = 9.71 P3 = 7.38 P4 = 86.26 Polarsation loss = 246% Initial Ei = 15kV/cm Final Ei = -9.37 kV/cm Time constant = 624 sec |
| +Pr N S C | P1 = 10.09 P2 = 6.6 P3 = 6.21 P4 = 47.76 Polarsation loss = 136% Initial Ei = *** Final Ei = -14 kV/cm Time constant = 975 sec |

within the measurement time window has been less than 65%. Also, the polarisation did not saturate till the end of measurement time. However, there were several samples, in which the polarisation decay was complete within our observation time itself. We choose one such sample (mentioned hereafter as Capacitor 3) to show the results of all four different cases of switching and non-switching of polarisation. The results of the measurements are given in Table 3.5. The complete backswitching of polarisation in the measurement time is observed in -Pr:S.C as shown in Fig. 3.15 and polarisation loss in this case is 246%. Though the backswitching has started in +Pr:N.S.C and +Pr:S.C as shown in Figs. 3.13 and 3.14, it is not complete in these cases within the measurement time. This is indicated by polarisation loss of less than 200% in these cases. In -Pr:N.S.C, the depolarisation is slow and polarisation

loss is 54%

On analysing the decay transients with TATS, we obtained well defined peaks

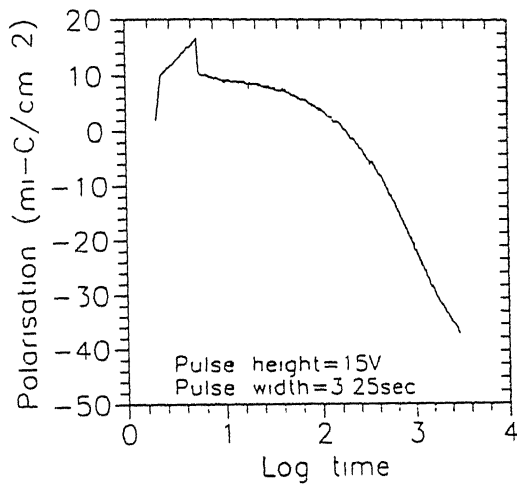


Fig 3 13 Depolarisation behaviour in +Pr N.S.C of Fast fired capacitor-3

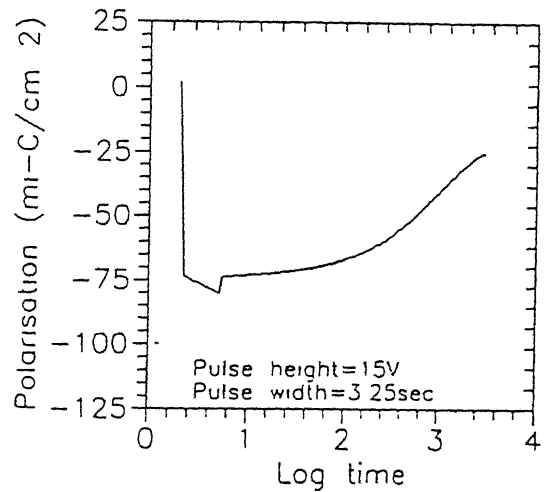


Fig 3 14 Depolarisation behaviour in +Pr.S.C of Fast fired capacitor--3

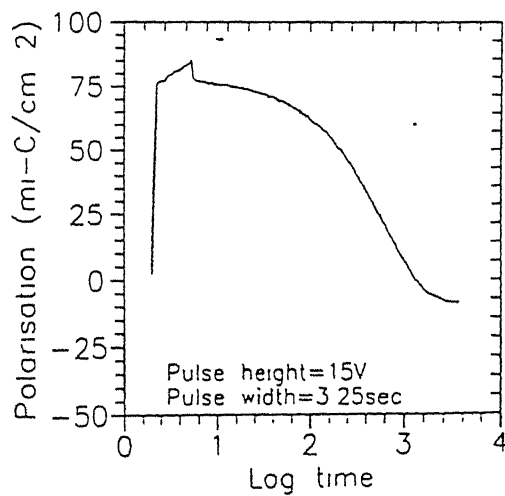


Fig.3.15 Depolarisation behaviour in -Pr.S.C of Fast fired capacitor-3

for all cases except for $-Pr: N S C$. where the decay process is slow The plot of $P(t) - P(2t)$ Vs $\log(t)$ for these three cases are given in Figs. 3.16-3 18. Transients

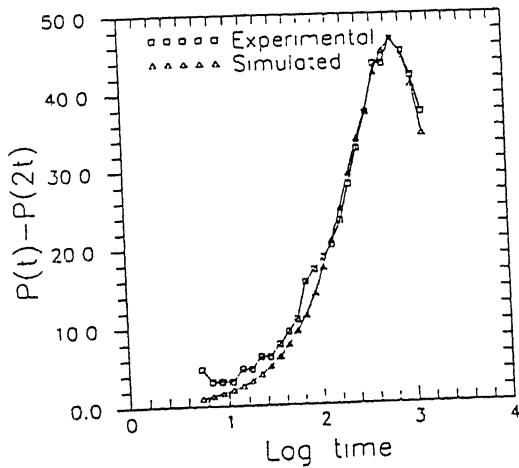


Fig. 3.16 TATS Signal for +Pr: N S C in Fast fired Capacitor3

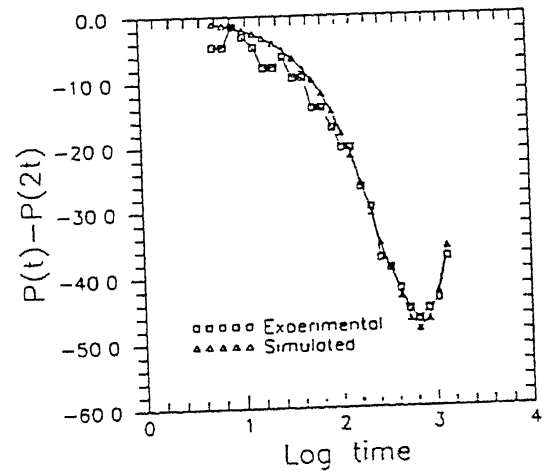


Fig. 3.17 TATS Signal For +Pr: S in Fast fired Capacitor3

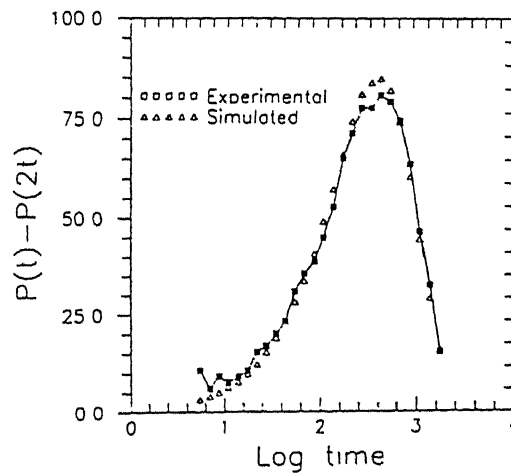


Fig. 3.18 TATS Signal For -Pr: S.C in Fast fired Capacitor3

simulated for exponential decay are plotted together with the experimental data for comparison. The decay process in all the cases are found to be exponential and time constant for the decay are obtained as discussed in the earlier sections. The time constant of the decay process for the above mentioned cases are given in Table 3.5.

3.5.4 Repeatability of Depolarisation Behaviour

The results presented so far clearly indicate that the depolarisation behaviour varies from one sample capacitor to another. In order to show the range of variations in the measured parameters in a single sample capacitor, we present the results of two runs of the depolarisation measurements, each run consisting of four cases of switching and non-switching of polarisation carried out on a sample (mentioned as capacitor-4). The behaviour of polarisation in the four cases of run1 is as shown in Figs. 3.19–3.22. The results of the measurements in run1 and run2 are given in Table 3.6 and 3.7. In the $-P_r$:S.C of Run1, the loss of polarisation is $77.32\mu C/cm^2$, i.e., the back switching of polarisation is complete in this case, which is indicated by the percentage of loss of polarisation being 208%. In the corresponding case in the run2, the loss of polarisation is 159% and in this case the backswitching is not complete. In $-P_r$: N.S.C. of Run1 and Run2, the rate of decay of polarisation is slow and hence the loss of polarisation in these cases is low. In $+P_r$: S.C. of Run1, saturation of polarisation is attained after a loss of $30.69\mu C/cm^2$. In the corresponding case in the Run2, even after a loss of $65.66\mu C/cm^2$, the saturation is not observed. The polarisation loss in $+P_r$: N.S.C. of both run1 and run2 are of nearly same value. The loss of polarisation in $-P_r$: N.S.C. is very small in both the runs. The time constant of decay in $-P_r$: S.C. in run1 is 1147s, while for corresponding case in run2 it is 1021s. The polarisation loss within the measurement time in the later case is less than the former. The time constant of decay in $+P_r$,

Table 3 6
Fast fired sample capacitor-4 Pulse height = 15 V
Width of the voltage pulse = 3 25 sec Polansation monitoring time = 1 hr

| | Case | Remarks |
|------|-----------|--|
| Run1 | -Pr S C | P1 = 85 09 P2 = 6 21 P3 = 8.15 P4 = 77 32 Polansation loss = 208% Initial Ei = 7 5 kV/cm Final Ei = -20 62 kV/cm Time constant = 1147 sec |
| Run1 | -Pr N S C | P1 = 6 6 P2 = 5 82 P3 = 6 99 P4 = 3 49 Polansation loss = 9% Initial Ei = 6 56 kV/cm Final Ei = 8 43 kV/cm Time constant = *** |
| Run1 | +Pr S C | P1 = 45 65 P2 = 3.1 P3 = 7 77 P4 = 30 69 Polansation loss = 82.94% Initial Ei = 16 87 kV/cm Final Ei = 17.81 kV/cm Time sonstant = 1616 sec |
| Run1 | +Pr N S C | P1 = 14 76 P2 = 4 66 P3 = 7 38 P4 = 22 53 Polansation loss = 60 89% Initial Ei = 17 81 kV/cm Final Ei = -18 75 kV/cm Time constant = *** |

Table 3 7
Fast fired sample capacitor-4 Pulse height = 15 V
Width of the voltage pulse = 3 25 sec Polansation monitoring time = 1 hr

| | Case | Remarks |
|------|-----------|--|
| Run2 | -Pr S C | P1 = 83.53 P2 = 4.66 P3 = 7 38 P4 = 59 06 Polansation loss = 159.62% Initial Ei = -24 37 kV/cm Final Ei = -31 87 kV/cm Time constant = 1021 sec |
| Run2 | -Pr N S.C | P1 = 9.71 P2 = 5 82 P3 = 6 99 P4 = 1 55 Polansation loss = 4% Initial Ei = -31 87 kV/cm Final Ei = 8.43 kV/cm Time constant = *** |
| Run2 | +Pr S C | P1 = 74.21 P2 = 2 33 P3 = 6 99 P4 = 65 66 Polansabon loss = 177.45% Initial Ei = 25 31 kV/cm Final Ei = 16 87 kV/cm Time constant = 1441 sec |
| Run2 | +Pr N S C | P1 = 13 98 P2 = 5.82 P3 = 7.77 P4 = 31 86 Polansation loss = 86.10% Initial Ei = 16.87 kV/cm Final Ei = -18 75 kV/cm Time constant = *** |

S.C. of run1 is 1616s and the time constant for the corresponding case in run2 is 1441s. Polarisation loss in the later case is more than the former. Hence we conclude

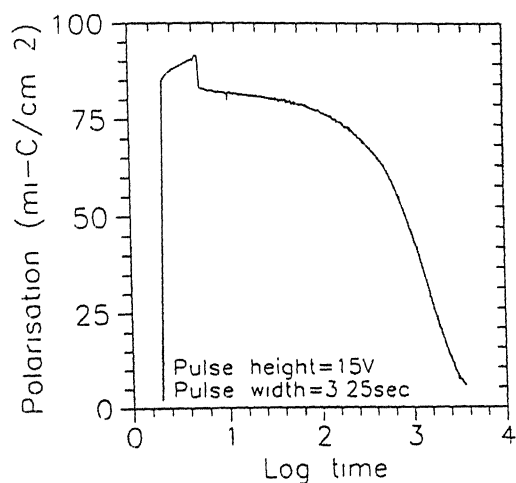


Fig 3 19 Depolarisation behaviour in -Pr S.C. of fast fired capacitor-4

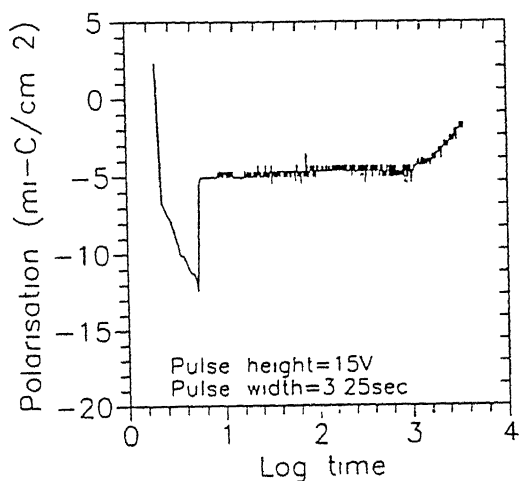


Fig 3 20 Depolarisation behaviour in -Pr N S.C. of fast fired capacitor-4

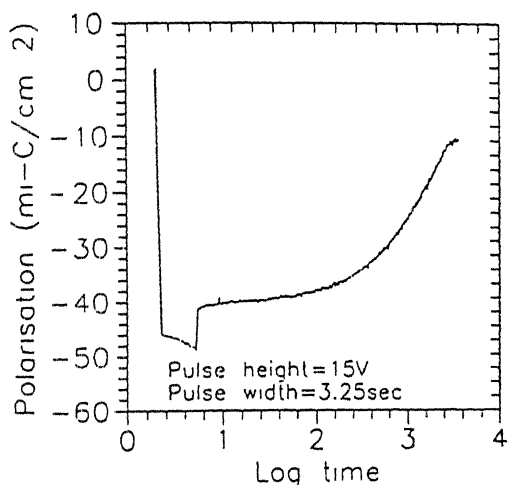


Fig 3 21 Depolarisation behaviour in +Pr S.C. of fast fired capacitor-4

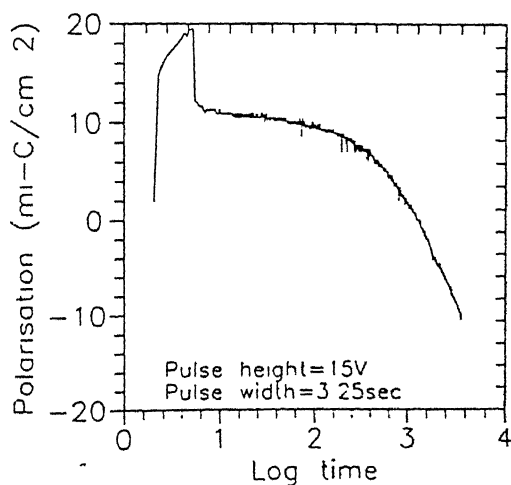


Fig.3 22 Depolarisation behaviour in +Pr N S.C. of fast fired capacitor-4

LIBRARY
I. I. T. KANPUR
No. A.122557

that though qualitatively the behaviour remains the same, there are variations in numerical values of the parameters. For, example the time constant ranges between 1000-1600s. These variations are most probably due to sensitivness of E_i to the measurement sequence. It is also noted that these variations in numerical values were more for those capacitors showing faster depolarisation i.e. backswitching phenomena.

3.5.5 Temperature Dependence of Depolarisation

One general feature of the depolarisation characteristics is that decay of polarisation in the depolarisation region is always exponential in nature. In order to detect any change in the rate of decay of polarisation at temperatures higher than room temperature, $-P_r \cdot S.C.$ is studied on a sample (mentioned as Capacitor-4), according to two different temperature schedules. In the temperature schedule-1, the sample temperature is increased throughout the measurement time and maximum temperature reached at the end is 88°C . The depolarisation characteristics with this temperature profile is is given in Fig.3.23. The small fluctuations in the polarisation

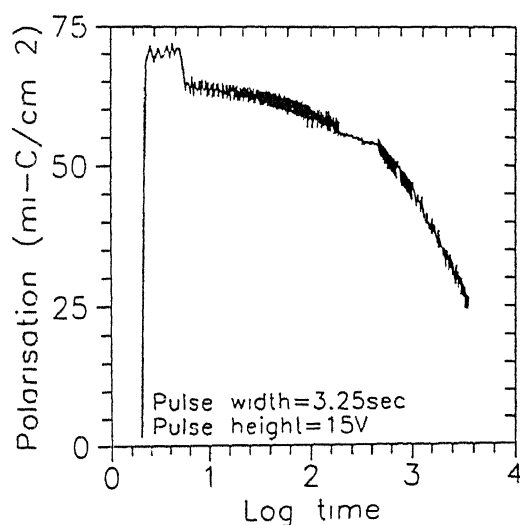


Fig.3.23 Depolarisation behaviour in $-Pr:S.C$ of Fast fired capacitor-4 with varying temperature

values throughout the measurement time is due to ac pickup from the thermocouple used for the temperature measurement. The above fact has been confirmed by doing the measurements without the thermocouple

In the depolarisation measurements with temperature schedule-1, since the measurements starts at room temperature, the initial E_i is recorded at room temperature. The time constant for the decay process is found to be 1818s. The loss of polarisation in this case is $42.74\mu C/cm^2$ and saturation of polarisation is not observed. The decay remains exponential in spite of continuous changes in temperature

In the temperature schedule-2, the temperature of the sample is maintained at $115^\circ C$, throughout the measurement time of one hour. Both the initial E_i and final E_f are recorded at $115^\circ C$. The behaviour of polarisation with time in this case is shown in Fig 3.24. In this case also the depolarisation characteristics is of same

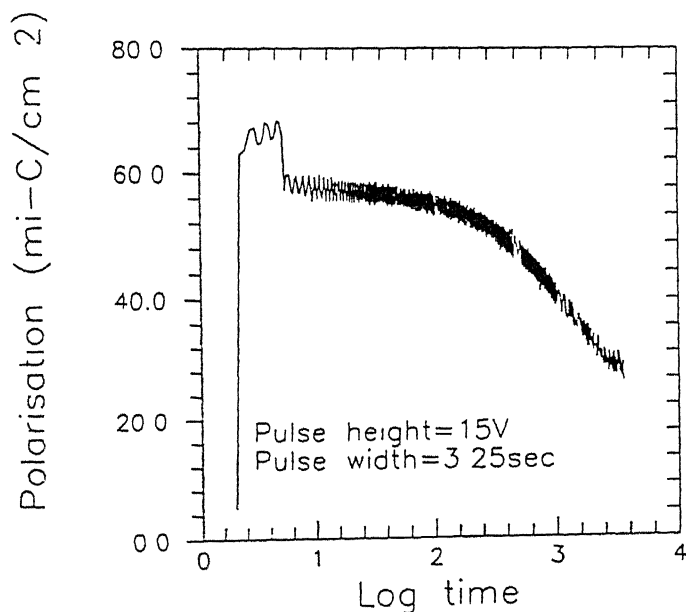


Fig. 3.24 Depolarisation behaviour in $-Pr:SC$ of Fast fired capacitor-4 at $115^\circ C$

Table 3.8
Temperature dependence of depolarisation
Fast fired sample · Capacitor - 4 · Pulse height = 15 V
Width of the voltage pulse = 3.25 sec · Polarsation monitoring time = 1 hr

| Case | Sample Temperature | Remarks |
|---------|---|--|
| -Pr:S C | Varied throughout Measurement Maximum T = 88 C | P1 = 68.38 P2 = 2.71 P3 = 7.95 P4 = 42.74 Polarsation loss = 133.56% Initial Ei = -29.06 kV/cm Final Ei = -14.06 kV/cm Time constnat = 1818 sec |
| -Pr:S C | Maintained at 115 C | P1 = 62.94 P2 = 2.71 P3 = 8.15 P4 = 31.47 Polarsation loss = 104.9% Initial Ei = 0.93 kV/cm Final Ei = -26.25 kV/cm Time constant = 1441 sec |

nature as that of the room temperature measurement. The small fluctuations in the values of polarisation throughout the measurement time is due to same reason discussed earlier. The time constant of the decay process in this case is 1441s. The results of the above two measurements are given in Table 3.8.

The time constant of the decay process with temperature schedule-1 is 1818s which is larger than the room temperature value by 670s. The time constnat for the decay process with temperature schedule-2 is larger than the room temperature value by 250s. But it is to be noted that a time constant difference of nearly same order is observed between the different cases of switching of polarisation in capacitor-4. Hence, the slow nature of decay with increase of temperature cannot be attributed to the high temperature since same behaviour is observed in room temperature values

also. The important point to be noted in the depolarisation measurements with temperature profile-1 is that even when the temperature is varied throughout the measurement the decay process is exponential. The possible reasons for temperature independence will be discussed in Chapter 4

3.6 Depolarisation Measurements on the Slow Fired Sample

The polarisation of the slow fired sample saturates at 25V and hence this voltage is chosen for the magnitude of the applied square voltage pulse. As discussed in the earlier section, the sample is polarised to the desired polarisation state by carrying out the P-E measurements on the sample at 25V. All the four cases of switching and non-switching of the previous polarisation state of the sample is carried out. The monitoring time of polarisation in the depolarisation measurements is 2000s. The depolarisation behaviour in different cases are given in Figs. 3.25–3.27. In +P_r, N.S.C the polarisation loss percentage is 182% and after this loss saturation of

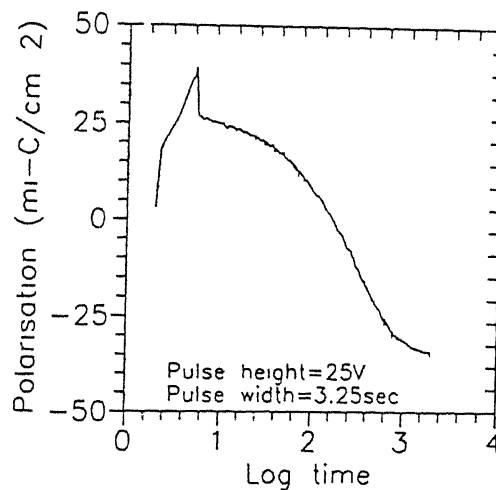


Fig. 3.25 Depolarisation behaviour in +P_r:N.S.C of slow fired sample

polarisation is observed In $+P_r$ S C after a loss of $57\mu C/cm^2$, the saturation

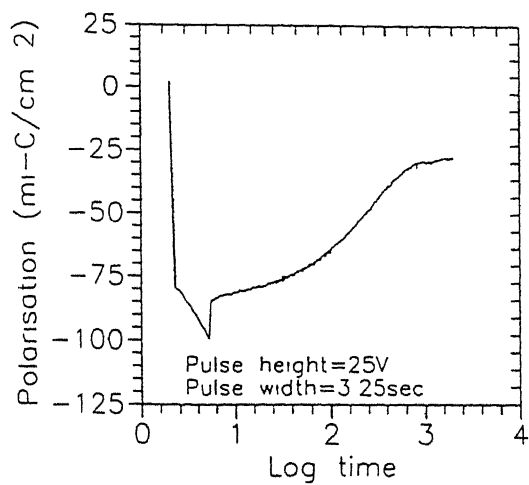


Fig. 3.26 Depolarisation behaviour in $+P_r$ S C of slow fired sample

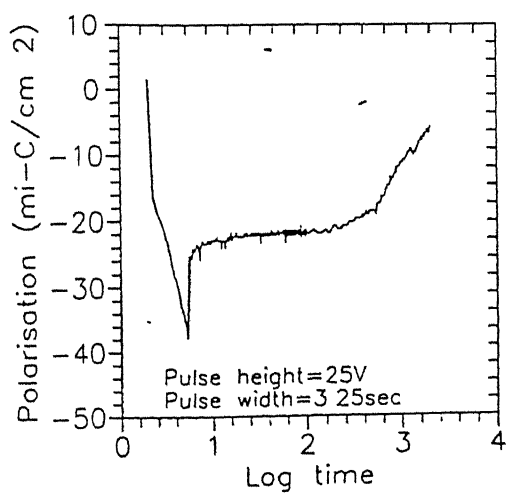


Fig. 3.27 Depolarisation behaviour in $-Pr:N.S.C$ of slow fired sample

Table 3.9
Slow fired sample Capacitor-A: Pulse height = 25V
Width of the voltage pulse = 3.25sec
Polarsation monitoring time = 2000sec

| Case | Remarks |
|----------|--|
| +PrN S.C | <p>P1 = 17.90 P2 = 21.26 P3 = 12.28 P4 = 62.10</p> <p>Polarsation loss = 182.14%</p> <p>Initial Ei = -20kV/cm Final Ei = -20 kV/cm</p> <p>Time constnat = 288 sec</p> |
| +PrS C | <p>P1 = 79.45 P2 = 20.14 P3 = 15.10 P4 = 57.07</p> <p>Polarsation loss = 167.85%</p> <p>Initial Ei = -20 kV/cm Final Ei = 6 kV/cm</p> <p>Time constant = 288 sec</p> |
| -PrN.S.C | <p>P1 = 16.22 P2 = 21.82 P3 = 12.86 P4 = 19.58</p> <p>Polarsation loss = 57.58%</p> <p>Initial Ei = -10 kV/cm Final Ei = 5 kV/cm</p> <p>Time constant = ***</p> |

of polarisation is observed. In both these cases the time constant for the decay process is 288s, which is three times less than that of the fast fired samples. In $-P_r$: N.S.C. the decay process is slow and hence the polarisation loss is low. In $-P_r$: S.C. last of our measurements on the sample, the sample gets shorted during the depolarisation measurements. It is indicated by the huge rise of polarisation of about $520\mu C/cm^2$ in the second region of the depolarisation characteristics. The rise is attributed to the presence of large leakage current. The hysteresis loop obtained after this measurement is distorted confirming the above fact. The results of the above measurements are given in Table 3.9.

It is generally observed that the slow fired samples get easily shorted during the electrical characterisation and this fact arises from the observation of frequent

shortings of slow fired samples in the P-E measurements. It is due to this reason the sample capacitor is damaged during the depolarisation measurements in the previous case. Hence, it is not possible to study the depolarisation behaviour with respect to other adopted experimental parameters like pulse height, pulse width and temperature.

3.7 Temperature and Electric field Dependence of Internal Bias E_i

In all the depolarisation measurements with respect to different experimental parameters there exists a common relation between the polarisation achieved in the depolarisation measurements and the final E_i . When the polarisation achieved is $-P_r$ (either by $+P_r$: S.C. or $-P_r$: N.S.C.), the final E_i is always found to be positive. Compared to the initial E_i , the movement of final asymmetry is towards the positive field axis. When the final polarisation achieved is $+P_r$, the behaviour is completely opposite. Hence, there exists a definite relation between the polarisation achieved and E_i movement.

In order to get more insight about the nature of E_i , it is studied as a function of applied electric field and temperature. Hysteresis loops are recorded on the sample by carrying out P-E measurements on the sample at different voltages from 10V to 40V and the corresponding values of E_i are calculated from the asymmetry of the hysteresis loop along the field axis. The results of the measurements are given in Table 3.10. The E_i values calculated at different field values are of same magnitude and hence it is clear that E_i is independent of applied electric field.

The E_i is also studied as a function of temperature. For this measurement, E_i is recorded at different temperatures on two sample capacitors (capacitor 4 & 5).

Table 3 10
Electric field dependence of Internal bias

| Applied Electric Field $E(\text{applied})$ (kV/cm) | Field due to Internal bias E_i (kV/cm) |
|--|---|
| 125 | 31.18 |
| 187.5 | 30.93 |
| 250 | 29.93 |
| 312.5 | 28.12 |
| 375 | 28.12 |
| 437.5 | 28.43 |
| 500 | 30 |

The results of the measurement are given in the Table 3.11. In the case of sample capacitor-5, initial E_i is negative and it's value found to increase with increase in temperature. In the case of sample capacitor-4. initial E_i is positive and it's magnitude is found to decrease with increase in temperature. The two sets of measurements can be summarised by noting that the $+P_r$ state becomes progressively more stable with increase in temperature. Another feature of this measurement is that coercive field E_c is also found to decrease with increase in temperature.

3.8 Influence of P–E Measurements on Internal Bias

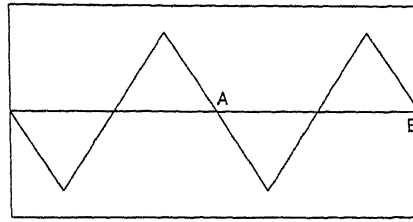
In all our measurements, the internal bias E_i is calculated from the asymmetry of the hysteresis loop along the field axis. But, we find that the values of E_i itself get

Table 3 11
Temperature dependence of internal bias
Fast Fired Sample: Capacitor -4

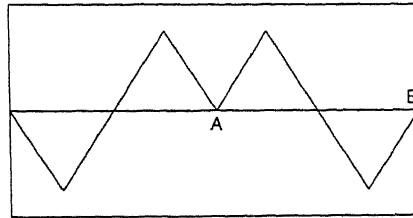
| Temperature (in K) | Ec (kV/cm) | Ei (kV/cm) |
|-------------------------|---------------|---------------|
| 303 | 83.43 | 17.81 |
| 323 | 77.81 | 14.06 |
| 343 | 72.18 | 12.18 |
| 363 | 67.5 | 9.37 |
| 388 | 64.68 | 10.31 |

Fast Fired Sample: Capacitor-5

| Temperature (in K) | Ec (kV/cm) | Ei (kV/cm) |
|-------------------------|---------------|---------------|
| 315 | 82.5 | -3.75 |
| 328 | 78.75 | -7.5 |
| 339 | 76.87 | -9.37 |
| 348 | 74.06 | -14.06 |



At point A $E_i = 16.87$ kV/cm
 At point B $E_i = 18.75$ kV/cm



At point A $E_i = 23.43$ kV/cm
 At point B $E_i = 9.37$ kV/cm

Fig. 3.28 Modulation of internal Bias E_i By P-E Measurements

influenced by the measurement sequence adopted for the P-E measurements. As discussed earlier in the Chapter 2, the voltage sequence used for P-E measurements are of triangular in nature and the measuring frequency is 0.4Hz. We measured the E_i values, without changing the measuring voltage sequence (points A and B in the Fig.3.28). The E_i obtained corresponding to point A is 16.87 kV/cm and at point B it is 18.75 kV/cm. Hence when the measuring voltage sequence is not changed, the change in the values of E_i is very small.

In the second measurement, we changed the measuring voltage sequence as shown in Fig. 3.28. The E_i values are recorded at points A and B. At point A E_i is 23.43 kV/cm and at point B it is 9.37 kV/cm. The change in measuring voltage sequence has changed the measured E_i value. But, it is to be noted that measuring voltage

sequence affects only the magnitude but not the orientation of E_i (in other words, the sign of E_i). The origin of variation of E_i will be discussed in the following chapter.

Chapter 4

Discussion

In order to study depolarisation phenomenon in ferroelectric capacitors, we have used a novel experimental sequence which has yielded new results and significant correlations. In a nutshell, our procedure was first to take the sample to desired polarisation state through application of external voltage, the sequence of which is same as that of one used in P-E measurements. Then, a square voltage pulse is applied to force the sample to either change it's existing polarisation state or to augment the existing state and then the remanent polarisation is monitored as a function of time in the absence of external voltage. Further, hysteresis loops are recorded before and after the measurements to detect possible changes in other electrical parameters such as E_c , E_i etc. Before discussing our model for the depolarisation characteristics we reiterate the three most important empirical facts (Cf.§Chapter 3).

1. Our result establishing the relationship between forced polarisation state and internal bias E_i shows that E_i helps in stabilizing a preferred polarisation state and E_i can be changed by application of external voltage. In other words, E_i *has the memory of the forced polarisation state*.

2. We also have shown that if time constant of decay is within the range of our monitoring interval, the sample polarisation not only decays, in fact it assumes the opposite polarisation state. This happens apparently in the absence of any external voltage. That is to say, depolarisation in these cases is not merely loss of polarisation but assumption of reverse polarisation state. Hence, *the depolarisation field must have a definite orientation that is opposite to the prepared polarisation state of the sample to force the sample to reverse it's polarisation state.*
3. From our transient spectroscopic analysis, we have found that the polarisation decay is exponential in nature. Hence, the strenght of the depolarisation field must be constant during the period of depolarisation.

If the depolarising field were dependent on the instantaneous value of spontaneous polarisation, then decay would be necessarily non-exponential for large values of change in the remanent polariation.

These three facts taken together help in building a possible model for origin of depolarisation. The exponential nature of the decay of polarisation rules out the involvement of either the standard capacitor used in the modified Sawyer-Tower circuit or any linear capacitor inside the sample in providing the depolarisation field, Since potential of any such capacitor would be time dependent reflecting the time dependence of polarisation, rendering the decay of polarisation non-exponential. Therefore, the depolarising field must be such that i) it is constant (time independent), ii) it responds to external field and iii) must have it's origin in the sample itself. Note that these are the observed characteristics of internal bias in the sample as well. Hence, we propose that internal bias itself is the most dominant source of depolarisation.

In order to aid the discussion of various cases studied in the last chapter, we introduce the following notation: Negative polarisation state $-P_r$ is represented as

;

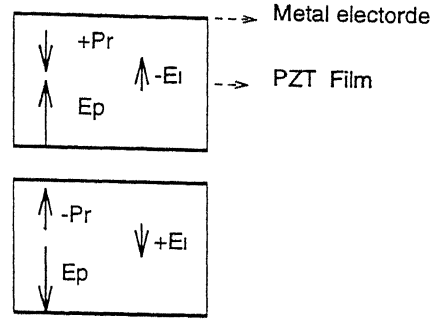


Fig 4 1 Schmeatic of orientations of
Polarisation and Internal Bias in the
absence of external Field

up arrow which is the direction of the external applied field to obtain this state and the corresponding electric field due to polarisation is oriented downward . Positive polarisation state is represented as an down arrow and corresponding field due to polarisation is oriented upwards. We already know from experiment that the internal bias is oriented in the direction opposite to the polarisation direction. This state can be represented pictorially as given in Fig. 4.1.

Clearly, in this configuration E_i , being opposite to the polarisation direction would try to reorient the domains in it's direction causing the observed depolarisation or polarisation reversal. The rate of depolarisation would then depend on the magnitude of E_i . Since the magnitude of E_i is smaller than the coercive field E_c in all cases, it is only to be expected that the polarisation reversal is extremely slow process[22, 23, 24]. More detailed discussion of time constant of decay will be taken up in a later section.

Recall that, E_i is connected to the prepared polarisation state. Hence, we assume that the origin of internal bias is such that it's orientation can be can be changed by the applied electric field. There have been reports of systematic observation of

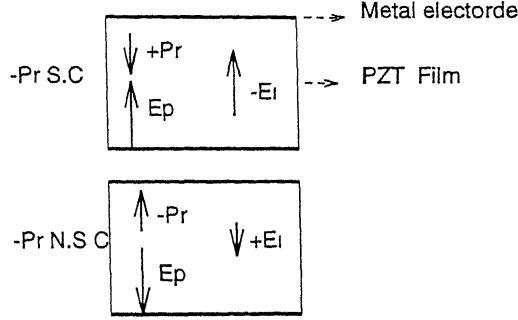


Fig 4.2. Schmeatic Showing Different Values of E_i

internal bias which has been attributed to the formation of defect dipoles mainly in the doped sample. The physical origin of defect dipoles will be discussed in a later section. We first show that orientation of internal bias leads to consistent explanation of all our cases studied in this work.

For example, in the $-P_r$:S.C. in run1 of capacitor-4, the achieved polarisation state is $+P_r$ and final E_i is negative. In this case, complete backswitching of polarisation state (from $+P_r$ to $-P_r$) is observed. When an external field is applied to switch the $-P_r$ state, the depolarisation field developed is in opposite direction to the applied field and the net polarisation is in the field direction. Once the field goes to zero, the orientation of the depolarising field and polarisation are as given in Fig. 4.2.

From the figure it is clear that the opposite field due to internal bias will reorient the domain polarisation. Depending upon the magnitude of internal bias there may be either loss or switching back of polarisation state during the measurement interval. In $-P_r$:N.S.C. in run1 of capacitor-4, the loss of polarisation is small and backswitching is not observed. This is due to the fact the value of E_i in this

case is small. This argument holds for all cases irrespective of the experimental parameters. The perusal of each case of measurement shows that there is qualitative agreement between the above scheme and occurrence of depolarisation. However, there are quantitative variations in the decay time constant and hence the amount of polarisation loss observed during the time window of observation. It varies from very small to 200 %. The former would be for a case where the value of E_i is small and in the later case it is large.

4.1 Critical Comparison of existing Models

In this section we compare the existing models of depolarisation field mentioned in the literature in the light of our results. The key argument of the three models are listed below:

1. Depolarisation is due to depolarising field from an interfacial capacitor inside the sample[10]
2. Depolarisation is due to depolarising field from the standard capacitor used in the depolarisation measurements. This model includes the possibility of depolarising field from the interfacial capacitor[8]
3. The existence of internal bias is correlated with defect dipoles and hence the defect dipoles should be considered as possible source of depolarising field.

4.1.1 Capacitor Models

According to the first model proposed by Benedetto et al, the depolarising field is attributed to the field due to presence of non-switching layers inside the film. In this model, even if the external field goes to zero the depolarising field represented as $E_d(t)$ appears in the film due to the charging of linear interfacial capacitor.

Benedetto et al argue that $E_d(t)$ is greater than coercive field E_c and the depolarisation process will stop once the $E_d(t)$ is equal to E_c . In their model they propose that the depolarising field at any instant of time is directly proportional to the remanent polarisation at that instant. Note that if $E_d(t) > E_c$, one expects very fast and non-exponential depolarisation. However this model would fail to explain the backswitching of polarisation, since the depolarising field becomes zero as the spontaneous polarisation decays to zero. Further, the occurrence of exponential decay over three orders of magnitude in time contradicts the expectations from this model. Benedetto et al do propose that the long time behaviour would be exponential but for only small changes in polarisation values. Recall that we observed 200% change in polarisation and yet the decay is exponential.

The second model to explain the depolarisation which is proposed by Mihara et al[8] is based on the depolarising field from the standard capacitor used in the depolarisation measurements. The working of this model is nearly same as that of interfacial capacitor model except for the fact that the interfacial capacitor is replaced by an external capacitor. But in our measurements, we found that rate of decay of polarisation is found to be independent of the voltage drop across the standard capacitor, since the voltage drop is itself very small. This model also suffers from the same problems as discussed for interfacial capacitor model. However, if the value of the standard capacitor is deliberately chosen to be low, as has been done by Mihara et al, its effect would certainly be noticed as has been observed by them. However, this would be a trivial source which can be avoided by simple changes in the memory cell design.

4.1.2 Defect Dipole Model

The existence of defect dipoles in the bulk PZT is proposed by many researchers, though the exact origin of it is not clear. Takahashi[25] studied the internal bias effects on the ageing properties of the lead zirconate titanate for a long time. He carried out an extensive study of internal bias in PZT, by doping the samples with donor (La,Nb) and acceptor (K,Fe) impurities. He observed that the internal bias effects are more predominant in samples doped with acceptor impurities compared with doping with donor impurities. The acceptor impurities have a valence less than that of the constituent atoms and hence while substituting for Ti^{4+} , they produce oxygen vacancies by valence compensation. He predicted the possibility of formation of the defect dipole complexes between the oxygen vacancies and acceptor impurities.

Lambeck et al[26] studied the ageing effects in $BaTiO_3$ single crystals doped with Mn. They observed the stabilisation of polarisation state which will lead to asymmetry along the field axis in the hysteresis loops. They attributed the stabilisation polarisation to the presence of defect dipole complexes (In this case $Mn^{2+} : Vo^{2+}$ associates).

Lohkamper et al[27] studied the growth of internal bias and decrease of internal bias by forced switching of polarisation by an ac field in Ni-doped $BaTiO_3$ single crystals. On the basis of their observation, they propose a model based on defect dipole complex $Ni^{2+} : Vo^{2+}$, to explain both the growth of internal bias and its decrease by forced switching.

Pike et al[28] studied the voltage offsets in PLZT thin films ($0.3\mu m$). The term voltage offset used by them represents the asymmetry along the field axis in the hysteresis loops. They observed that the voltage offsets are changed by applying a dc bias to the sample and then either heating the sample or shining UV light on the sample. Though they attribute the voltage offsets to the presence of defect dipoles

inside the sample (in this case defect dipole complexes consists of lead and oxygen vacancies), the explanation for the phenomenon of is based on the trapping of charge carriers

However, even if the existence of defect dipoles does explain the existence of internal bias, it would fail to explain the fact that the depolarisation field is time independent. If the external voltage is able to orient the defect dipoles, so would be the internal electric field due to spontaneous polarisation in the absence of the external voltage.

4.1.3 Proposed Model For Depolarisation

From the foregoing discussion, it is amply clear that the none of the existing models would be able to provide a cogent explanation of exponential backswitching of the polarisation state. We have seen that the depolarising field developed in response to the applied field is in the direction opposite to the net polarisation and should remain constant in the absence of the external field Hence, we propose that the origin of the depolarising field and internal bias lies in the space charge layers at the interface. The requirement then is that the net charge developed in the space charge region on application of applied field is such that the field developed is opposite to the external field. For example, in a particular case, the space charge configuration may be as shown the Fig. 4.3.

Further, the charge developed must be immobile so that the field due to domain polarisation is unable to make them move. This points to the involvement of immobile species such as lead vacancies. On the basis of these clues, it is now possible to develop a scenario concerning the origin of the space charge.

Scott et al[29] studied the effects of space charge regions on the electrical characterization of the PZT thin films prepared by the sol-gel technique. They carried

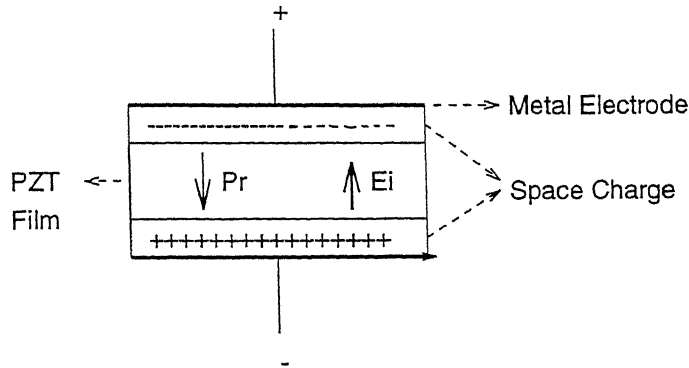


Fig. 4.3. Schematic showing
Origin of Depolarising Field

out Auger measurements to find out the variation of oxygen vacancy concentration normal to the film. The results of the measurement are reproduced in Fig. 4.4. It can be noted from this data that the oxygen concentration is not the same throughout the film: Rather it decreases sharply near the metal electrodes. It drops to approximately 50% of its value in the center of the film, while still 20nm from the Pt surface. This creates an oxygen deficient region that may be n-type in contrast to p-type PZT throughout the interior of the film. The oxygen deficient regions are present near both the electrodes.

The interfacial region in all probability also contains lead vacancies formed during the high temperature processing. Hence, it is reasonable to assume that the likelihood of occurrence of defect associates between lead and oxygen vacancies is quite high in these regions. Recently, Pike et al[28] invoke their presence in interpreting their results on voltage offsets in hysteresis loops. It is also quite well known in the literature that electrically, metal-PZT interfaces act as Schottky diodes. Hence, the presence of a space charge region at the interfaces due to the Schottky barrier is but natural. On application of external voltage, one of the Schottky barriers gets

SURFACE LAYER AND
CONTACT INTERFACE

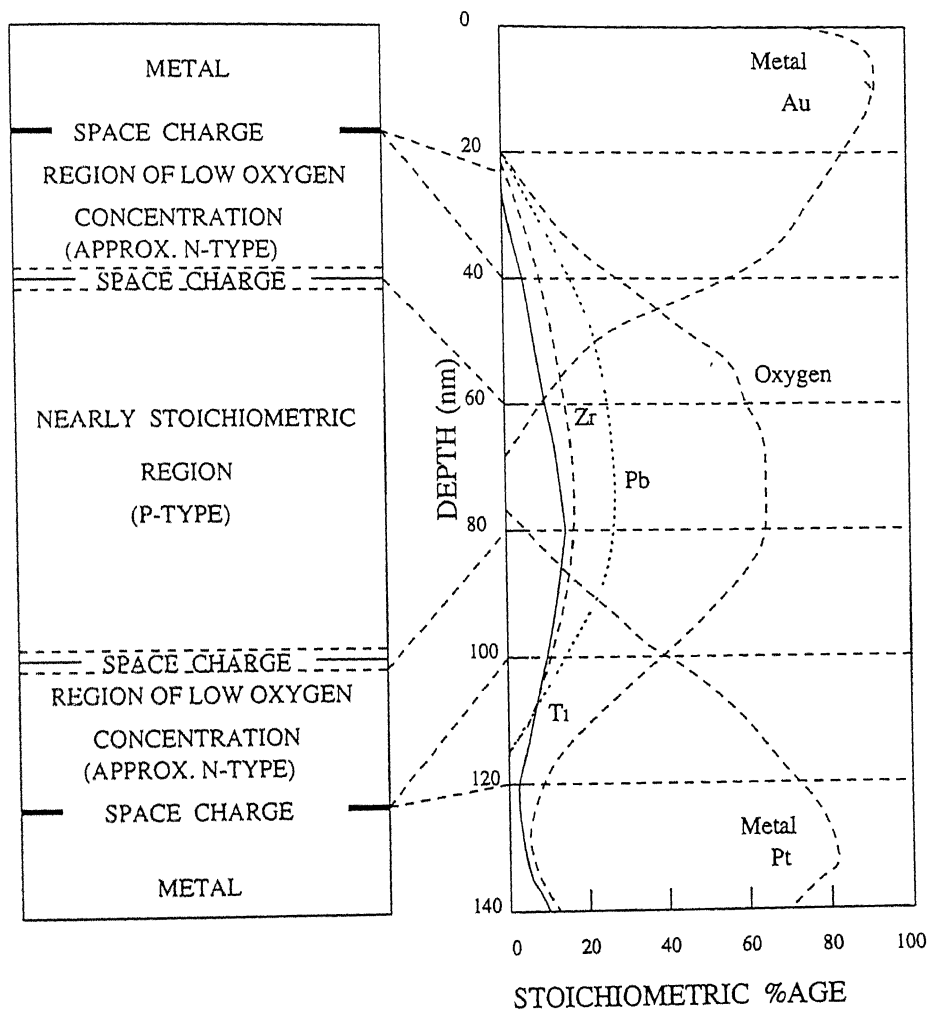


Fig. 4.4 Auger Microprobe Data For PZT Film With Pt and Au electrodes (Ref:Scott et al)

forward biased and the other reverse biased. We propose that the defect-associates get charged due to trapping of carriers in the forward bias junction and detrapping occurs in the reverse biased junction. For example a $Pb^{--} - O^{++}$ defect can develop negative charge on capturing of an electron which gets injected when junction gets forward biased. Hence, a negative space charge would be produced next to the positive electrode for the applied bias as shown in Fig. 4.3, if we consider the interfacial region to be n-type. More detailed studies are required to identify the exact nature of the trapping sites and the trap energy associated with it. Most likely the defect dipole associates are mid gap acceptors, communicating with the conduction band.

A quantitative study of depolarisation time constants and its relation to the measured internal bias is at present difficult. Though, our internal bias measurements provide qualitative guide quite well, the measured values can have large uncertainties. In the last chapter we have shown that the measured value of internal bias depends crucially on the sequence of voltage applied to measure hysteresis. This can be either due to progressive partial charging of the traps in the space charge region or movement of free charges such as oxygen vacancies. Careful measurements with high frequency hysteresis loops are required to remove this ambiguity. Note that typical frequency of our hysteresis loop measurement is 0.4Hz. Hence, the measurement process itself in part can modify the internal bias. A high frequency hysteresis loop measurement is at present being set-up in our laboratory to overcome this difficulty.

However, undoubtedly the maximum internal bias in our sample is in the range of 30-40kV/cm. Scott et al and others have established that there exists an activation field of the order of 600kV/cm for polarisation switching. Hence, the observation of slow depolarisation in our experiments is in qualitative agreement with field activated switching.

The independence of depolarisation behaviour on the pulse height and pulse width arise from the fact that the internal bias values are not affected by these parameters. This has been confirmed by our experiments. The value of the internal bias remain unchanged upto applied field values of 500kV/cm. The capture and emission time constants are probably faster than the time scales of applied voltage in this work and hence the independence of of depolarisation behaviour on pulse width. More detailed studies of trap kinetics as a function of temperature, specially at lower temperature, is necessary to ascertain the pulse height and pulse width dependence.

The depolarisation decay characteristics remains exponential even when temperature is increased from 300K to 350K during the depolarisation measurements. This indicates that depolarising fields does not change significantly in this temperature range. The observed time constants at different temperatures also do not show any systematic change and remains at the values observed at room temperature. The switching of polarisation though field activated, is not expected to be significantly temperature dependent below Curie temperature. However, the measurement of internal bias at different temperatures does show systematic changes as already presented in Table 3.11. It shows that keeping the measurement frequency same, the internal bias shift towards negative field values with increasing temperature. This means that application of cyclic voltage (0.4Hz triangular) is making the +Pr state more stable at higher temperatures. This may be due to asymmetry in the nature of the Schottky contacts of the sample. Recall that the two metal contacts are prepared from very different process steps. Also, note that this needs to be investigated with high frequency measurements, since the very process of measurement of E_i most likely changes it as discussed earlier. We believe that the systematic changes observed in E_i with temperature is more an indication of effect of frequency

on hysteresis measurements, rather than changes in absolute value of E_i developed during pulse voltage application. This we infer from independence of decay time constant of depolarisation at different temperatures.

Chapter 5

Summary and Conclusions

Thin films of ferroelectric lead zirconate titanate (PZT) have many potential applications including that of non-volatile random access memory in computer systems. However, there are at present several problems relating to the electrical properties of these films such as fatigue, depolarisation and imprint which are not well understood. In this work we systematically study the depolarisation behaviour or loss of polarisation in absence of external voltage in sol-gel derived PZT thin films.

Crack free films of $Pb_{1.05}(Zr_{0.53}Ti_{0.47})O_3$ with thickness in the range of $0.8 - 1.25\mu m$ have been prepared using modified sol-gel technique on Pt substrates. Two different heating sequences, as developed by Majumder et al. in our laboratory, were employed. Films which are fired at $400^\circ C$ and annealed at $700^\circ C$ are termed as the slow fired and which are fired at $600^\circ C$ and annealed at $700^\circ C$ are termed as fast fired films.

Routine characterization of the sample have been carried out using several techniques including XRD to confirm the formation of the perovskite, P-E hysteresis measurements to check the ferroelectric nature and Capacitance- Voltage measurements to determine the dielectric constant of the films.

The depolarisation behaviour of PZT thin films have been studied using a new measurement sequence which consists of following steps: i) Polarising the sample to the desired polarisation state utilising the P-E measurements ii) Switching or reinforcing the polarisation state by applying a square voltage pulse and iii) monitoring the remanent polarisation as a function of time. P-E measurements have been carried out at various steps to observe the possible changes in loop parameters. The depolarisation characteristics have been measured with respect to pulse height(15 and 20V), pulse width (3.25-30.25sec) and temperature according to two schedules. Some of the significant observations and conclusions of this work are listed below.

1. The hysteresis loops obtained from the PZT capacitors exhibited asymmetry along the field axis, indicating the presence of internal bias E_i which favours a definite polarisation state in the sample. It is observed that this internal bias can be changed by external voltage pulse and this has been confirmed by demonstrating definite relationship between the achieved polarisation state and the final orientation of E_i .
2. In our measurements, we not only observed the loss of polarisation but also backswitching of polarisation states. i.e. the sample capacitor reverts back to it's polarisation state which was assumed prior to application of voltage pulse forcing it to change the sign of remanent polarisation.
3. We used an isothermal technique called time analysed transient spectroscopy(TATS) to analyze the polarisation decay transients. It is found that the decay of polarisation is exponential with respect to time. The decay process with time constants less than 2000secs are determined using TATS.. There is sample to sample variation of the observed time constants which is most probably due to the inhomogeneous distribution of species responsible for producing the depolarising field.
4. The decay process is generally much faster in slow fired films then in the fast

fired films. The slow fired films have a tendency to electrical shorting after a few cycles of measurement.

5. From the exponential nature of the decay of polarisation, it has been concluded that the value of the opposing depolarising field remains constant in the absence of the external voltage.
6. The result of our depolarisation measurements with respect to pulse height, pulse width and temperature indicated that depolarisation behaviour is independent of these experimental parameters.
7. It is found that the values of internal bias E_i obtained from low frequency hysteresis measurements (0.4Hz) are influenced by the measurement sequence itself. However, it is observed that the orientation of E_i is not affected by the P-E measurements.
8. We considered three existing models and found that they are unable to explain the crucial observations of our measurements such as exponential nature of polarisation decay and backswitching of polarisation states.
9. We propose a new model based on the depolarising field arising from the asymmetry of charge distribution in the interfacial space charge regions due to trapping (detrapping) of charge carriers while applying an external voltage pulse. The exponential backswitching of polarisation state is attributed to the large and constant values of E_i which gets developed at the interfacial layers. The trapping sites are most probably due to immobile defects such as lead vacancy–Oxygen vacancy complexes.

5.1 Scope For Future Work

On the basis of our results, we suggest that this work can be extended along the following lines:

1. High frequency P-E measurements can be made to quantify the relationship between internal bias and depolarisation.
2. Our measurements can be extended to wider temperature range and small pulse widths.
3. Similiar measurements can be carried out in doped ferroelectric PZT films, especially in acceptor doped films. Such measurements would help in quantitative elucidation of mechanisms underlying depolarisation and its relationship with internal bias.

Bibliography

- [1] C. Feldman. *Rev. Sci. Instr.*, **26**, 463(1955).
- [2] A. Moll. *Z. Angew. Phys*, **10**, 463(1958).
- [3] E.K. Muller, B.J. Nicholson, and G.E. Turner. *J. Electrochem. Soc.*, **110**, 969(1963).
- [4] J.F. Scott, L. Kammerdiner, M. Paris, S. Traynor, V. Ottenbacher, A. Shawabkeh, and W.F. Oliver. *J. Appl. Phys.*, **64**, 787(1988).
- [5] David Bondurant. *Ferroelectrics*, **112**, 273(1989).
- [6] J.F. Scott and A.D. Araujo. *Science*, **246**, 1400(1989).
- [7] T. Mihara, H. Watanabe, and C.A.P. Araujo. *Jpn. J. Appl. Phys.*, **33**, 3996(1994).
- [8] Tkahashi Mihara, Hiroyuki Yoshimori, Hitoshi Watanabe, and Carlos A. Paz de Araujo. *Jpn. J. Appl. Phys.*, **34**, 2380(1995).
- [9] T. Mihara, H. Watanabe, and C.A. Araujo. *Jpn. J. Appl. Phys.*, **32**, 4168(1993).
- [10] J.M. Benedetto, R. A. Moore, and F.B. McLean. *J. Appl. Phys.*, **75**, 460(1994).
- [11] C.B. Sawyer and C.H. Tower. *Phys. Rev.*, **35**, 269(1930).

- [12] T. Hase and T. Shiosaki. *Jpn. J. Appl. Phys.*, **30**, 2159(1991).
- [13] T. Katayama, M. Sugiyama, M. Shimizu, and T. Shiosaki. *Jpn. J. Appl. Phys.*, **31**, 3005(1992).
- [14] H. Kidoh, T. Ogawa, H. Yashima, A. Morimoto, and T. shimizu. *Jpn. J. Appl. Phys.*, **31**, 2965(1992).
- [15] Chi. Kwok, S.B. Desu, and D.P. Vijay. *Ferroelectric Letters*, **116**, 143(1994)
- [16] M. Sayer. *Con. Ceram. Quart*, **21**, 59(1990).
- [17] R. C. Mehrotra. *J. Non. Cryst. Solids*, **121**, 1(1990).
- [18] Guanghua yi and Michael sayer. *Ceramic Bulletin*, **70**, 1173(1991).
- [19] R. Schwartz, B. Bunker, D. Dimos, and R. Assink annd D. Tallantandi. *Ferroelectrics*, 1991.
- [20] S.B. Majumder, D.C. Agarwal, Y.N. Mohapatra, and V.N. Kulkarni. *Integrated Ferroelectrics*, **9**, 271(1995).
- [21] A.M. Lines and Glass. *Principles and Applications of Ferroelectrics and Related materials*. Clarendon Press, Oxford, 1977.
- [22] D.J. Taylor, P.K. Larsen, and R. Cuppens. *Appl. Phys. Lett*, **64**, 1392(1994).
- [23] H. Ishikawa. *Jpn. J. Appl. Phys.*, **32**, 442(1993).
- [24] J.C. Burfoot and G.W. Taylor. *Polar dielectrics and their applications*. Macmillan, London, 1979.
- [25] Sadayuki Takahashi. *Ferroelectrics*, **41**, 143(1982).

- [26] P.V. Lambeck and G.H. Jonker. *J. Phys. Chem. Solids*, **47**, 453(1986).
- [27] R. Lohkamper, H. Neumann, and G. Arlt. *J. Appl. Phys.*, **68**, 4220(1990).
- [28] G.E.Pike, W.L. Warren, D. Dimos, B.A. Tuttle, R. Ramesh, J. Lee, V.G. Keramidas, and J.T. Evans. *Appl. Phys. Lett.*, **66**, 484(1995).
- [29] J.F.Scott, C.A.Araujo, B.M.Melnick, L.D.McMillan, and R.Zuleeg. *J. Appl. Phys.*, **70**, 382(1991).